

**SIMULATION AND OPTIMISATION OF A FULL DEEP DRAWING  
PROCESS**

**By  
Mathews Kaonga**

A thesis submitted in fulfillment of the requirements for the degree of Master of  
Engineering in Production Engineering and Management

**The University of Zambia**

October 2009

## **ABSTRACT**

All sheet metal forming processes occur after permanent plastic deformation resulting in the material properties changing and therefore it is necessary to determine the extent to which a material can further be deformed for subsequent forming operations. Traditionally, experimental trial and error procedures have been employed to determine these changes and adjust process settings (dies, loadings, tool path) accordingly. However, this approach is time consuming and depends heavily on the experience of the tool designer. To address these shortcomings, sheet metal forming simulations have been applied instead. Although this alternative approach has gained acceptance in industrial sheet forming, most simulations are done on individual forming processes. This dissertation demonstrates the use of simulations to couple the forming processes by using Forming Limit Diagrams. Experimental verifications were performed to validate simulation results.

Blanking, deep drawing and bending processes were independently modeled using SolidWorks 2005 and simulated using Cosmosworks 2005. The workpiece material used was AISI 1023 carbon steel. For all simulations, the dies and punch were assumed to be rigid bodies made from alloy steel. The forming loads were determined using finite element analysis. The forming loads and the assessment of the forming limit for the material were obtained using contour plots of the stress and strain respectively.

The location of the critical areas on the workpiece that were obtained by using contour plots of the stress and strain for the blanking, deep drawing and bending simulations were in good agreement with the theory and experimental

results. The results obtained from coupling deep drawing and bending processes showed that the processes are the major strain contributors in a production line. Blanking has less or no impact on subsequent processes.

### *DEDICATION*

*To my family.*

## ACKNOWLEDGEMENTS

First and foremost I thank the almighty GOD, for having finally made this humble effort a reality.

I would like to express my deepest gratitude to my supervisors Dr. Levy Siaminwe and Dr. Henry M. Mwenda whose support, stimulating suggestions and encouragement helped me during the time of research and writing of this thesis. Without their invaluable guidance and persistent help, this work would have never been possible.

I sincerely appreciate Mr. Mwape Chileshe and Mr. G. Chizyuka for all their help, support, interest, valuable hints and enjoyable friendship. In addition, special thanks are due to Mr. Lawrence Ng`andwe who helped me with experimental work.

Finally, I wish to express my warm gratitude to my wife Fridah, my sons Sangwani and Walusungu for their ongoing support and heaps of love that made it possible for me to undertake the graduate studies. I love them so much.

## TABLE OF CONTENTS

	<b>Page</b>
ABSTRACT	I
DEDICATION	lii
ACKNOWLEDGEMENTS	Iv
TABLE OF CONTENTS	V
LIST OF FIGURES	Vii
LIST OF TABLES.	Viii
NOMACLATURE	X
<b>CHAPTER 1: INTRODUCTION</b>	
1.1 Introduction	1

1.1.1 Sheet Metal Forming	4
1.2.1 Forming Process Simulation	5
1.2 Problem Statement	9
1.3 Research Objective	11
1.4 Research Justification	11
1.5 Research Approach	12
<b>CHAPTER 2: FULL DEEP DRAWING PROCESS</b>	
2.1 Introduction	13
2.2 Full Deep Drawing Process	13
2.3 Blanking Process	14
2.4 Deep Drawing Process	16
2.5 Bending Process	18
2.6 Spring Back	20
<b>CHAPTER 3: METHODOLOGY</b>	
3.1 Introduction	21
3.2 Computer Models and FEA Simulations of Forming Processes	21
3.2.1 Input Data for Simulations	23
3.2.2 Simulation Procedure	23
3.2.3 Meshing	24
3.3 Modeling of a Blanking Process	24
3.3.1 Blanking Simulation Procedure	26
3.4 Deep Drawing Simulation	26
3.4.1 Modelling of a Deep Drawing Process	27
3.4.2 Deep Drawing Simulation Procedure	28
3.5 Modelling of a Bending Process	29
3.5.1 Bending Process Simulation Procedure	30
3.6 Optimization Procedure	30
3.6.1 Deep Drawing Optimization Procedure	30
3.6.2 Objective Formability Function	31
3.6.3 Forming Limit Diagram (FLD)	32

3.7 Experimental Verification	36
3.7.1 The Vremac Hydraulic Press	36
3.7.2 Experimental Procedure	37
3.7.3.1 Deep Drawing Process	38
3.8 Coupling Simulations	38
<b>CHAPTER 4: RESULTS</b>	
4.1 Introduction	40
4.2.1 Blanking Simulation Results	40
4.2.2 Bending Simulation Results	42
4.2.3 Deep Drawing Simulation Results	44
4.3 Experimental Verification Results	46
4.3.1 Blanking Process Experimental Results	47
4.3.2 Blanking: Experimental Versus Simulation Results	48
4.3.3 Deep Drawing Experimental Results	49
4.3.4 Comparison of Experimental and Simulated Deep Drawing Results	49
4.3.5 Bending Process	50
4.3.6 Experimental Results of The Bending Process	51
4.3.7 Bending : Experimental Versus Simulation Results	52
4.4 Full Process	53
4.4.1 Experimental Results of the Full Forming Process	53
4.4.2 Deep Drawing	53
4.4.3 Bending	54
4.4.4 Blanking	55
4.4.5 Coupling Simulations	56
<b>CHAPTER 5: DISCUSSION</b>	61
5.1 Introduction	61
5.2 The Blanking Process	62
5.3 The Deep Drawing Process	64
5.4 The Bending Process	65
5.5 Coupling Simulations	65

CHAPTER 6: CONCLUSIONS AND RECOMMENDATIONS	67
6.1 Conclusions	67
6.2 Recommendations	67
REFERENCE	68
APPENDICES	73

## LIST OF FIGURES

	<b>Page</b>
Figure 2.1 Blanking Process	15
Figure 2.2 Deep Drawing Process	17
Figure 2.3 Edge Bending Process	19
Figure 3.1 Finite Element Model of a Blanking Process	25
Figure 3.2 Deep Drawing Solid Model	28
Figure 3.3 Edge Bending Simulation Model	29
Figure 3.4 Diagrammatic Representation or Regions of Formability Assessment	33
Figure 3.5 Typical Forming Limit Diagram	35
Figure 3.6 The Vremac Hydraulic Press.	37
Figure 4.1 Contour Plots for a Blanking Process	41
Figure 4.2 Graph of Punch Force against Displacement for a Blanking Process	42
Figure 4.3 Contour Plots of Bending Process	43
Figure 4.4 Graph of Simulated Punch Force against Displacement for a Bending Process	44
Figure 4.5 Contour Plots of a Deep Drawing Process	45
Figure 4.6 Simulated Punch Force Against Punch Displacement for a Deep Drawing Process.	46
Figure 4.7 Punch Pressure/Displacement Against Time for a Blanking Process.	47
Figure 4.8 Punch Force Against Displacement During Blanking Process.	48
Figure 4.9 Pressure/Displacement Against Time for a Deep Drawing Process.	49
Figure 4.10 Punch Force Against Displacement for a Deep Drawing Process.	50
Figure 4.11 Punch Pressure/Travel Against Time for a Bending Process.	51
Figure 4.12 Bending Punch Pressure Against Time	52

Figure 4.13	Experimental/Simulation Punch Force Against Displacement for a Bending Process	52
Figure 4.14	Comparison of Punch Forces	54
Figure 4.15	Comparison of Blanking Forces	55
Figure 4.16	FLD of Major against Minor Strain in a Blanking Process	56
Figure 4.17	FLD Showing Major against Minor Strains in a Deep Drawing Process	57
Figure 4.18	FLD Showing Major Strain Against Minor Strain in a Bending Process	57
Figure 4.19	Combined FLD of a Blanking and Deep Drawing Process	58
Figure 4.20	FLD of Deep Drawing against Bending Process	59
Figure 4.21	FLD of Combined Blanking, Deep Drawing and Bending Process	60

## LIST OF TABLES

	<b>Page</b>
Table 3.1 Mechanical Properties of 1023 Carbon Steel	22
Table 3.2 Geometrical Properties of a Blanking Process	24
Table 3.3 Tool and Process Parameters for a Deep Drawing Process	27
Table 3.4 Geometric Properties of a Bending Properties	29

## NOMENCLATURE

A	Area
B	Blank outer radius
X	Blank inner radius
C	Constant
E	Young's modulus
D	Outer diameter
d	Inner diameter
F	Force
FEA	Finite Element Analysis
FEM	Finite Element Method
FLD	Forming Limit Diagram
k	Work hardening factor
$\tau$	Shear stress
$\sigma$	Stress
$\varepsilon$	Strain
t	Thickness
L	Length

## CHAPTER 1

### INTRODUCTION

#### 1.1 Introduction

Sheet metal forming is one of the most widely used manufacturing processes in industry that is used to change the geometry of sheet metal of typically about 6mm thickness without loss of material. This wide use can be attributed to the ease with which a wide range of products can be produced using the method, coupled with its adaptability to new manufacturing technologies such as hydro forming [Gokhale, 2002].

Sheet metal forming operations consists of simple bending, ironing, wheeling, press brake forming, stretch forming, roll forming, rubber-pad forming, stamping, flanging, spinning, embossing, bulging, hyperplastic forming, peen forming, explosive forming, magnetic-pulse forming and deep drawing of complex parts [Kalpakjian and Schmid, 2008]. The commonest sheet metal forming process is deep drawing and is frequently used in the automotive, packaging and home appliances/kitchen utensil producing industries. Examples of deep drawn automotive components include outer car body panels, inner car body panels, fenders and stiffeners. The common products for packaging that are made using sheet metal forming processes include pet food containers, beverage containers and toe cups. Some home appliances and kitchen utensils that are produced using sheet metal forming include kitchen sinks, pots and pans.

The objective of sheet metal forming processes is primarily to produce a desired shape by plastic deformation. The final product quality is dependant on both the sheet material characteristics and process variables such as strain, strain rate and temperature [Gedney, 2002]. These variables are influenced by the tool and die design, blank geometry, properties of the lubricant used (such as

coefficient of friction and heat capacity) and drawing speed. A deviating product shape can result if incorrect combinations of these process parameters are used. A deviating shape is usually caused by elastic spring back of the job after forming and retracting the tool.

During forming, the forces and the properties of the workpiece material are of concern to the design engineer. The material properties of the sheet being formed change and affect the process parameters during processing. For example, a full deep drawing process which comprises blanking, deep drawing, trimming, hemming and flanging would have the blank material properties altered during and at the end of each of these forming processes. It is precisely because of this that the design of a full deep drawing process still depends on the knowledge and experience of the tool design engineer, wherein the selection of values for the various process parameters is based on trial and error methods.

Since sheet metal forming leads to plastic deformation of the sheet material below its recrystallization temperature, this usually leads to an increase of the strength and hardness of the material at the expense of ductility [Hosford, 1983]. Therefore, determination of the extent to which a material can deform is necessary in order to design a functional sequence of forming operations.

Generally, sheet materials exhibit different deformation behaviour in different directions because of the rolling processes used in their production. These directional or orthotropic properties of sheet materials are a result of mechanical fibering or preferred orientation in the rolled sheet material [Leu, 1997]. This orthotropy has an effect on both the forming load and the product quality, as is evident in the latter case with the formation of 'ears' in a cylindrical cup drawing and in the former case when sheet metal is bent in the direction parallel to the rolling direction [Dieter, 1988]. The presence and magnitude of friction during forming also influences the forming processes. The magnitude of friction is dependant on the absence or presence of lubricant and its characteristics, the presence of coatings of impurities on the sheet metal blank, surface roughness

of the tool and the blank, blank holder pressure and process velocity [Danckert, 2004].

It is therefore important to have a good knowledge of the influence of all the aforementioned variables on sheet metal forming process in general and on the deep drawing process in this work, if a proper tool design is to be achieved. If this knowledge is lacking, then after selecting a tool suitable for design the blank material and choosing an appropriate lubricant, an extensive and time consuming trial and error process is undertaken to determine the proper tool design and all other variables leading to the desired shape [Park and Colton 2005]. The trial and error process may require an unnecessary number of deep drawing strokes before settling on an acceptable design, or may even require redesigning of the expensive tools. In order to reduce on this time wasting and costly exercise, process modeling for computer simulations can be used in place of the experimental trial and error process.

This research work was conceived from the problems Zamcapitol Enterprise Limited of Lusaka, Zambia was facing in their sheet metal forming production lines. The main problem with the sheet metal forming production lines at the enterprise was identified to be lack of accurate tool design that resulted in deviating products. This was primarily a result of failure to evaluate the amount of formability remaining in sheet material as it passed from one forming process to the other in the production lines. Furthermore, the enterprise was still using the traditional trial and error tool design that relied heavily on the experience of the tool designer.

Simulation based design approaches have been used for forming processes. Using similar approach, a full process simulation and optimisation was undertaken in the present work. The work done here involved computer simulations of the forming processes to evaluate the amount of strain and stress each forming process contributed to the final product. Forming loads were also determined from the simulation for each process. Thereafter, the simulation results were experimentally verified using a Vremac Press which had in it the Angela system, an integral data capturing unit.

### **1.1.1 Sheet Metal Forming**

Sheet metal forming is used to produce various products from mild steel, stainless steel, copper, aluminium, gold, platinum, tin, nickel, brass and titanium. To reduce costs and increase the performance of manufactured products, more and more lightweight and high strength materials have been used as a substitute to the conventional steel. These materials usually have limited formability, thus, a thorough understanding of deformation processes and the factors limiting the forming of sound parts is important, from both engineering and economic viewpoints.

In sheet metal forming, a piece of material is plastically deformed between tools to obtain the desired product. Sheet metal forming is characterised by the conditions in which the stress component normal to the plane of the sheet is generally much smaller than the stresses in the plane of the sheet.

The common defects that occur in sheet metal forming are wrinkling, necking, scratching, cracks, stretcher strains and orange peeling. Wrinkling occurs in areas of high compressive strains and necking in areas with high tensile strains. Scratching is caused by defects on the tool surface and orange peel may occur after excessive deformation depending on the grain size of the material [Menders, 2003].

In sheet metal forming operations, the amount of useful deformation is limited by the occurrence of unstable deformation which mainly takes the form of localized necking or wrinkling. Failure by wrinkling occurs when the dominant stresses are compressive, tending to cause thickening of the material. Localized necking occurs when the stress state leads to an increase in the surface area of the sheet at the expense of a reduction in the thickness. The two kinds of neck that occur are diffuse necking (so called because its extension is much greater than the sheet thickness), and the localized necking (through thickness

thinning), which is terminated by final separation or fracture. After the localized neck initiates, further deformation of the material concentrates in this localized region, and homogeneous deformation away from neck region vanishes completely. The localized neck is therefore a very important phenomenon in determining the amount of useful deformation that can be imposed on a workpiece. The mechanism for initiation of localized band involves a number of factors including material properties and punch profile. The phenomenon is attributed to the softening effect, including geometric softening (the decrease with strain of the cross-section area which bears the forming load, the generation of voids), and material softening (flow stress decreases with the increase of the effective strain).

### **1.1.2 Forming Process Simulation**

Since sheet metal forming is an attractive subject to die designers and production engineers due to its wide application, many investigations have been carried out in an attempt to obtain optimal operating parameters that could result into the desired shape.

Picart [1995] developed an implicit algorithm based on the Newton-Raphson scheme used to solve the non-linear equilibrium of the blanking process and corresponding constitutive equations in a blanking process. In this research an uncoupled approach by fracture or damage criteria was developed and the coupled approach by Gurson and Lemaitre models thereafter incorporated to describe the occurring damage mechanism and predict crack initiation.

A considerable amount of research has been done on modeling and analysis of bending simulations. This includes analytical, empirical and Finite Element Analysis (FEA) of various bending processes.

Chuan et al. [1993] developed mathematical models for plain-strain sheet bending to predict springback, bendability, strain and stress distributions and the maximum loads on a punch and a die. Vin and Streppel [1996] developed 'three section' model for air V-bending. The material behaviour was described in

this work by Swift's equation while the change of Young's modulus under deformation was addressed by Streppel. Leu [1997] reported that precise prediction of the springback and bendability were the key factors influencing the design of bending tools, controlling the bending process and assessing the accuracy of part geometry. Date et al. [1999] developed a process model to assess the effect of different geometric and material parameters on the springback in the air V-bending process. Jenn-Terng and Kinzel [2001] investigated the influence of the Bauschinger effect on springback in sheet metal forming. Inamdar et al. [2000] performed experiments to study the effect of geometric parameters on springback in sheets of five different materials for air V-bending.

Xuechun et al. [2002] performed FEA springback simulations of V free bending, using a self developed two-dimensional elasto-plastic finite element program. The material model considered was linear hardening and had an elasto-plastic power-exponent for the change of Young's modulus during deformation. Gantner and Bauer [1999] undertook FEA simulation of complex bending processes using a nonlinear simulation program and suggested it is the best solver for crash analysis and simulation. Rahul and Haldar [2003] reported the effect of anisotropy on springback using FEA. Analytical models were then developed to crosscheck the trends predicted by FEA. They concluded that the higher the anisotropy, the higher the springback. The FEA results generated in this work further showed that minimum springback occur for isotropic material.

Despite its apparent simplicity, deep drawing of a cylindrical cup is a very complicated process that has attracted a lot of research work, as it involves setting a lot of process parameters in order to produce a desired product. Attempts to analyze the process and to evaluate the drawing forces have been made by many researchers. The early work of Siebel and Pomp [1932] and separately by Sachs [1934], laid the foundation for the subsequent theoretical treatment of the problem. The radial drawing problem was first studied by Hill [1950] who considered the limiting cases of plane stress and strain. A comprehensive study of the elementary mechanics of the drawing process was carried out by Chung and Swift [1951] who improved the model for bending over

the die profile radius. They were, however, unable to extend their solution to the punch nose region. The attempts to develop a simple method for the estimation of the drawing force were continued by Stoughton [1960] and later by Panknin [2000].

Numerical methods used in deep drawing process simulations were studied by Chiang and Kobayashi [1966] and separately by Budiansky and Wang [1966] in their application to the analysis of the radial drawing problem of anisotropic materials.

The analysis was extended into the punch nose region by Woo [1996] who also improved the formulation of the blank holding pressure boundary condition. The variation of stress with sheet material thickness was taken into account by Odell [1973] who concluded that the membrane theory was adequate when cups of moderate die radius/material thickness ratios were analyzed.

With the developments of fast, high volume and stable FEA programs, coupling simulations have also received attention in the recent past. Several methods have been developed and a lot of different approaches tried over time to couple forming simulations with subsequent processes of interest, with varying levels of success measured against their ability to conform to practical results. The results from this research are able to predict formability with close conformity to practical situations.

Seo [2002] investigated the work hardening of the material during multiple forming. The thrust of his work was on the loss of ductility due to cumulative work hardening during multiple deep drawing. A three-dimensional model was used to conceptualize the design necessary to set up finite element models. The results of his work showed that work hardening induced from the first draw station affects material deformation behaviour in subsequent forming. The aim of the investigation was to predict material fracture upon reaching a final shaping station.

Jain et al. [2003] conducted simulations on the progressive-die-sequence design for automotive parts. The objectives of their investigation were to determine the number of forming stages, tool geometry for each stage, drawing depth in each forming stage and the blank holder force for each stage. They concluded that the integration of simulations and past experience can reduce the number of die tryout tests and associated time and cost. Furthermore, they concluded that integrating simulations allows further refinement and optimization of the die design to improve product properties such as wall thickness tolerances.

Gaier et. al [2004] developed an algorithm for integrating the forming simulation of sheet metal and fatigue life prediction for application in the design of automotive structures. The focus of the work was on the distribution of the effective strain resulting from forming simulations that were taken as input for fatigue analysis. This work was carried out using different material parameters that included the fatigue limit, yield strength and cyclic stress-strain curve.

Ghouati and Chen [2006] proposed different possibilities to be included in the closed loop design and optimization simulation of sheet metal forming. The goal of their work was to develop a coupling algorithm of forming simulations and product performance simulations. Their algorithm enabled transferring of the forming simulation results to crash, durability models taking into account the difference in modeling.

Brunssen and Wohlmuth [2006] proposed a method for reducing computational costs in FEM simulations of incremental metal forming processes in order to circumvent the need for sophisticated re-meshing procedures. The focus was on developing a coupling algorithm for simulation of incremental elastoplastic forming processes which involved small but very mobile forming zones and non-linear contact problems.

The concept of analysing material undergoing multiple forming processes using Forming Limit Diagrams (FLDs) has been extensively studied as well. A study of failure in biaxially stretched sheets by Keeler and Backofen [1985] resulted into

the development of (FLDs). The main discovery in this work was that the largest principal strain before any localized thinning in a sheet increased as the degree of biaxiality increased. Several materials were tested including steel, copper, brass and aluminium sheets, by stretching them over solid punches. Later, Keeler [1988] found that the material properties have a great effect on the strain distribution in biaxial stretching of sheet metal. He pointed out that when the material work-hardening exponent,  $n$ , is higher, the strain distribution will be relatively homogeneous. To the contrary, materials having lower  $n$  values develop sharp strain gradients with deformation (strain) concentrations in very small regions, thus causing premature failure. He constructed a map in principal strain space ( $\epsilon_1$ ,  $\epsilon_2$ ) which separated safe strain states that a material could safely withstand from the more severe strain states which would lead to failure. By definition,  $\epsilon_1$  is the major principal strain, and  $\epsilon_2$  is the minor principal strain. This work illustrated that FLDs identified the combination of major and minor in-plane principal strains beyond which failure occurs. With further development of the experimental techniques by Goodwin and Tsang [1986], a FLD for mild steel was obtained which served as a criterion for most stamping processes. Stemming from the contribution of Keeler [1988] and Goodwin and Tsang [1986] to the understanding of material formability, the developed FLDs for carbon-steel stamping are often referred to as Keeler-Goodwin diagrams. The FLDs cover strain states for uniaxial tension through plane strain to balanced biaxial tension.

Though experimental methods have been widely applied to solve production problems in the sheet metal industry, Gandhi et al. [2005] reported that there has been intense research to develop theoretical FLDs in order to better understand material forming limit diagrams and to effectively apply theoretical predictions to the actual design of sheet metal forming processes.

## **1.2 Problem Statement**

It is evident that extensive theoretical and practical research work has been done on blanking, bending and deep drawing of different sheet materials. Generally, the research has been centered on analysing the stress and strain

distribution of a formed product and evaluating the forces and the factors affecting the forming processes. The work hardening of the material during sheet metal forming, in particular multiple deep drawing, has been done to predict material fracture at the last draw station. Forming Limit Diagrams have been used to assess the formability of the material by separating the safe and unsafe strained regions that would lead to failure. However, the literature review has shown that all the reported studies have analysed the different forming processes independently even though in practice a sheet material normally undergoes blanking, bending and deep drawing before a desired shape is achieved. Analysing forming processes independently neglects material properties changes and would not assist in tool design in a case where a sequence of forming processes is involved. Therefore, a link between each forming stage must be established if an accurate forming tool is to be designed.

It can also be deduced from the foregoing literature survey that there is a trend towards the incorporation of computers in the design and manufacture of formed sheet metal products. The literature survey shows that sheet metal forming processes have been simulated and analysed using various packages such as Autoform, LS Dyna, Abaqus, Ansys and Cosmoworks. The software are able to simulate the forming processes independently with good accuracy based on the material property data input. The literature review has further underlined the improvements of product quality and the savings in terms of time and money, accruing from the use of computers in design and manufacture of formed metal products. Besides the foregoing, it is a fact today that complex features can now be manufactured with the aid of computers that could otherwise be impossible to make using conventional methods.

In Zambia the use of computer assisted design and manufacturing is still in its infancy despite the availability of software on the market. Zamcapitol Enterprise Limited, a sheet metal forming company, for example has until recently totally relied on the trial-and-error method in their die design and manufacturing process. It has, however, had to contend with problems of maintaining product quality and dimensional tolerance, as well as product failure while on the production line due to an inability to determine the remaining formability of the

product through the forming processes done in the company plant. With these problems the company had no option but to embrace computer-aided engineering in order to remain competitive.

While FEA serves well for die design and optimisation, it faces unique challenge for process design and optimization for each particular product. Suggestions have been made that at the product development stage, it is possible to model and analyse the whole production process before physical prototyping. With FEA all possible flaws in the production line can be identified and corrected at the design stage.

It is necessary to determine the stress/strain state of the sheet metal at every forming stage for easy assessment of formability or work hardening of the material.

### **1.3 Research Objective**

The main objective of this research was to accurately simulate and optimize the blanking, deep drawing and bending processes of sheet metal, specifically AISI 1023 carbon steel and to subsequently link them together depending on the process requirements. This was expected to enable tool designers to numerically evaluate the sheet metal forming tool and process design and to then enable redesign where necessary in order to meet the requirements of producing desired shapes using these coupled processes.

The specific objectives were to:

1. Simulate blanking, deep drawing and bending processes of mild steel grade AISI 1023 sheets.
2. Experimentally verify the simulated sheet metal forming processes.
3. Couple the simulated processes in order to develop a full process simulation.

### **1.4 Research Justification**

The alternative to simulation, the trial-and-error method of die and process design, is costly and time consuming as it involves many tryouts during which experience is relied upon solely to fix any flaws that are encountered. In order to increase efficiency in die design and process design FEA can be used as an alternative simulation tool to the traditional, costly and time consuming trial and error methods.

Deep drawing typically faces difficulties or challenges associated with wrinkling, thinning, fracture and optimization of shapes, all of which are expensive as they lead to wastage of material and loss of production time. Simulation can predict such defects during product development and often prevent their occurrence during production with the attendant saving time and material, by identifying necessary and often times simple changes in design. It is of importance therefore, for sheet metal fabricating companies to adopt product development simulation techniques in order to reduce or eliminate the aforementioned problems and thus remain competitive.

## **1.5 Research Approach**

The main benefits offered by full process simulation in sheet metal forming is the identification and correction of flaws in the production line prior to manufacture in order to cheaply and efficiently produce the desired product. The cost of die production is also reduced because the simulation replaces the expensive traditional trial and error procedure of producing dies.

The work reported here was carried out in the following three phases:

- First, FEA models were developed representing the physical processes of blanking, bending and deep drawing. Optimization of each process was achieved by varying their respective process parameters followed by re-runs until acceptable results were obtained. Acceptable results were determined by ensuring that the strains fall within the forming boundaries.

- Then experimental verification was done using a Vremac Hydraulic Press incorporating within it the Angela system, a data capturing unit.
- Finally the linking or coupling of all three simulations was done.

## **CHAPTER 2**

### **THE FULL DEEP DRAWING PROCESS**

#### **2.1 Introduction**

Most sheet metal products undergo a series of metal forming processes before a desired shape is obtained. These forming processes can be grouped into two major categories, cutting and forming operations [Sharma, 2003]. The cutting operations include blanking, punching, notching, perforating, trimming, slitting and lancing. Forming operations include: bending, flanging, deep drawing, redrawing, hemming and squeezing. The deep drawing process is always accompanied by bending and blanking. A series of forming processes would constitute a full forming process.

#### **2.2 The Full Deep Drawing Process**

Deep drawn products in modern industries usually have complicated shapes that require several successive operations to be achieved. The first process that a sheet metal undergoes is usually blanking, the shaping of the sheet metal to optimal size. This is followed by the deep drawing process, after which trimming of the resulting flange is done in order to remove the ears from it to ensure uniformity of the flange shape on all sides of the final product. These ears are often wavy projections or unevenness formed along the edge of the flange or end of the wall of the cup. These are formed due to uneven metal flow in different directions, which is primarily a result of the presence of planar anisotropy in the sheet.

Die design for a full deep drawing production line becomes a challenge if a lengthy and expensive prototype testing and experimentation is used in arriving

at a final competitive product. The overall quality and performance of the product formed depends on the distribution of strains in the sheet material. In addition, the material properties, geometry parameters, machine parameters and process parameters affect the accurate response of the sheet material to mechanical forming of the component as the blank passes from one forming stage to the other.

In cutting operations, the work piece is stressed beyond its ultimate strength. The applied force induces enough shearing stresses to cause crack initiation in a sheet metal and eventual rupture or separation. In forming operations on the other hand, the stresses are always below the ultimate strength of the sheet metal. There is no cutting of the sheet metal therefore, but rather only the contours of the workpiece are changed to obtain the desired product.

In this work, blanking was simulated as it is frequently used, and was taken to be representative of other sheet metal cutting process. Deep drawing and bending processes were simulated here and were taken to be representative of forming operation. The forming sequence of the full deep drawing process under study comprised blanking, deep drawing and bending processes.

### **2.3 The Blanking Process**

Blanking is a metal forming process, through which a metal workpiece is removed from the primary metal strip or sheet when the former is punched out. In a blanking operation the piece punched out, called the blank, is the required product of the operation. The operation is usually the first step in a series of operations. Figure 2.1 shows a die/punch arrangement for the blanking process. The punch has the same shape as that of the die opening except that it is smaller on each side by an amount known as clearance. The sizing of the clearance is very important in the blanking operation and is a function of the material thickness and material properties. The clearance determines the shape and quality of the sheared edge.

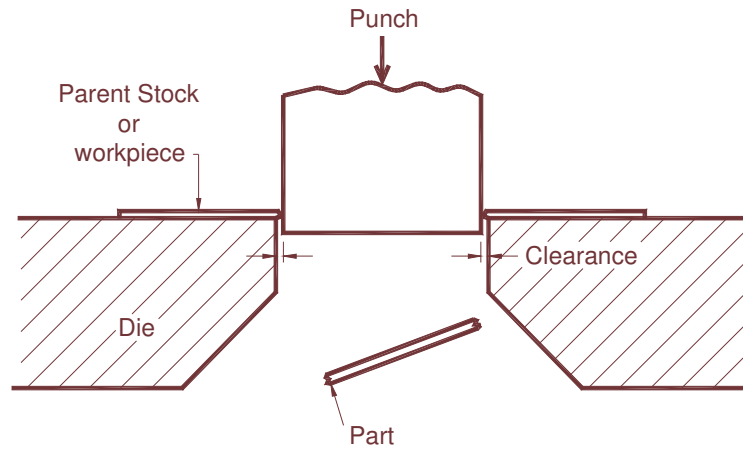


Figure 2.1: The Blanking Process

As the punch touches the material and travels downwards, it pushes the material into the die opening creating a deformation zone around the punch-die area where the material is subjected to both tensile and compressive stresses. These stresses are highest at the edges of the punch and die which therefore defines the point where cracking commences. [Sharma, 2003].

In a blanking process, the material undergoes three stages of deformation. The elastic stage during which sheet metal is compressed and deformed slightly between the punch and die, stress and deformation levels do not exceed the material elastic limit. In the second stage the material undergoes plastic deformation at the edges where the punch penetrates into it. In the final stage, the penetrating punch further strains the material until it reaches the fracture limit leading to micro cracking and separation of the blank away from the parent sheet.

After the cutting operation has been completed, elastic recovery of the strip material takes place on release of the blanking pressure, whereby the blank expands slightly. The blanked part is therefore eventually actually larger than the die opening through which it was produced. This difference in size that is a result of elastic recovery depends on the blank size, thickness and material type. A blanked edge is normally characterized by the four attributes that include burnish, burr, fracture and roll-over.

During the blanking process, the punch force changes as the workpiece is deformed, strain hardens and separates. The punch force increases as the punch is pressed against the workpiece resulting into deformation of the latter, and then decreases as the workpiece separates into two pieces.

During the blanking process, the cutting action initially creates compressive strains around the deformation zone which as the cutting action continues, become reversed to tensile strains, finally changing into shear strains, leading to eventual break through the thickness of the material and separation.

After blanking the top surface exhibits rollover which is followed by a burnished area, which leads to the first of two fractures, caused by tensile strains across the cutting edges of the die and punch steels. These are separated by a small secondary burnish area.

Finally, there is a burr hanging down in the direction of the cutting action. Mild steel work hardens, and the action of trimming results in hardened pieces breaking off as the burr is formed.

## **2.4 The Deep Drawing Process**

Deep drawing is a compression-tension forming process. In this process a flat sheet metal blank is formed into a cylindrical part by means of a punch that presses the blank into a die cavity with a small radial clearance, typically of 2mm. Although the process is called deep drawing, meaning deep parts, the basic operation also produces parts that are shallow or have moderate depth. A two-dimensional deep drawing illustration is shown in Figure 2.2.

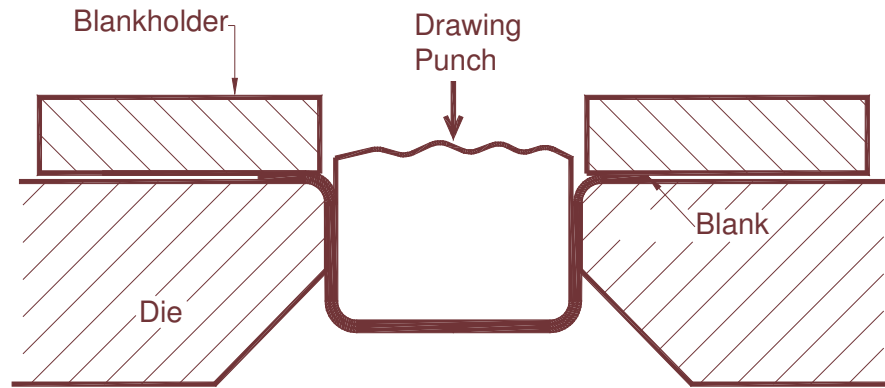


Figure 2.2: Deep Drawing

An initially flat or pre-shaped sheet material, the blank, is clamped between the die and the blank holder. The blank holder is loaded by a blank holder force, which is necessary to prevent wrinkling and to control material flow into the die cavity. Then the punch is pushed into the die cavity, simultaneously transferring the specific shape of the punch and the die to the blank. During the forming stage the material undergoes both compressive and tensile deformation at the die entry region.

The material flow into the die cavity is controlled by the blank holder. A restraining force is created by friction between the tools and the blank. The friction between the tools and the blank is influenced by the blank holder force, lubrication or coating on the blank or tools [Menders, 2003].

In deep drawing, wrinkling may occur in the flange area when the minor stress in the sheet is compressive. Wrinkling of the flange areas can be suppressed by the blank holder force. However, wrinkling may also occur in unsupported regions or regions in contact with only one tool. A compressive hoop stress may arise in the unsupported areas if too much material is allowed to be drawn into the cavity [Grieve, 1996]. The usual remedy is to increase the blank holder force which in turn leads to an increase in the radial stress and strain, the former which is defined by the relationship

$$\frac{\sigma}{1.1\sigma_y} = \ln\left(\frac{b}{x}\right) \dots\dots\dots \text{Equation 1}$$

Where  $\sigma_y$ ,= material yield stress,  $b$  =blank outer radius and  $x$  = blank inner radius. [Rowe, 1977]. The lateral hoop contraction arising from the stress which is defined by the expression [Rowe, 1977]

$$\left(\frac{\sigma}{1.1\sigma_y}\right) = 1 - \ln\left(\frac{b}{x}\right) \dots\dots\dots \text{Equation 2}$$

accompanying this radial stretch helps alleviate the hoop compression. The wrinkling tendency is also affected by elastic modulus and thickness of the sheet metal, as well as the tooling. It is important to note that the outer radius of the blank decreases continuously as the drawing process continues [Rowe, 1977].

In deep drawing process, the drawing force increases from zero up to a maximum value and then falls steadily to a minimum value. The base is first formed and then the actual drawing process follows.

Limitations of the deep drawing process depend on the properties of the sheet material, lubricant, tool geometry and forming parameters. The upper process limit is characterised by the formation of tears. The lower limit is characterised by the tendency to build folds. These two failure criteria then define the limits of the process. The limiting draw ratio is a measure of the process limit due to tearing. The limiting draw ratio can be increased by minimising the punch force and by increasing the tearing factor.

## 2.5 The Bending Process

All sheet metal forming operations often incorporate some form of bending feature. It is a very common forming process for changing sheet into various shapes. In a sheet metal production line, bending is encountered when flanging or hemming. The most commonly used bending processes are edge bending

and V-bending. Figure 2.3 shows a two-dimensional drawing of the edge bending process. In V-bending, a wedge-shaped punch forces the metal sheet into a wedge shaped die cavity. In edge bending, a flat punch forces the stock against the vertical face of the die. The bending axis is parallel to the edge of the die and the stock is subjected to cantilever loading. To prevent movement of the die and the stock during bending, it is held down by a pressure pad before the punch contacts it and during forming.

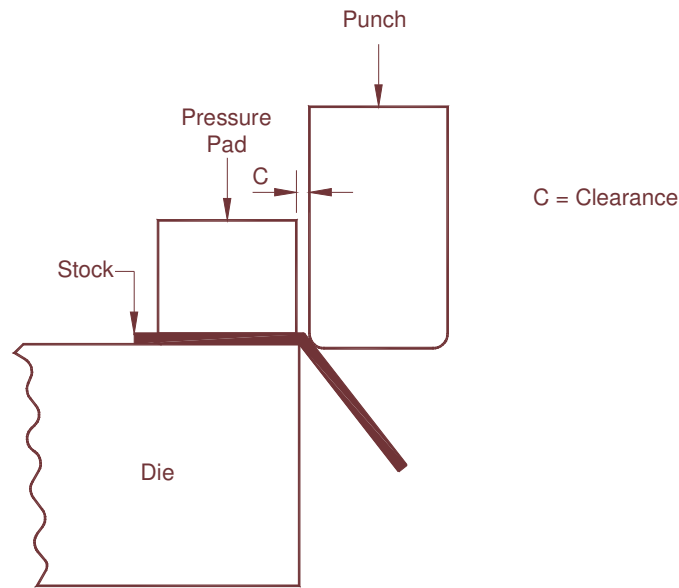


Figure 2.3: The Edge Bending Process

During the bending process, the outer surface of the sheet material is in tension and the inner surface in compression. If the bend radius is too sharp, excessive tensile strain on the outer surface may cause failure. The bend radius must be small enough however, in order to bring much of the sheet cross section into a state of plastic flow. If the proper ratio of the minimum bend radius to the thickness is not observed, then localized necking or fracture occurs [Grieve, 1996].

The major process parameters that influence the bending process are the dies, punch travel and control of the bend angle. Accurate bending allowances and

springback predictions are important to maintain the geometric tolerance of the finished part.

## **2.6 Spring Back**

After the bending operation is complete, when the pressure on the sheet metal is released, there is an elastic recovery or spring back by the material. This elastic spring back causes a decrease in the bend angle. To compensate for spring back in edge bending, the part is over bent by an angle equal to the spring back angle, which implies that the bending die angle does not therefore correspond precisely to the angle desired for the workpiece. The ratio of the imposed bend angle to the final angle is referred to as the spring back factor. Spring back may also be eliminated by applying plastic deformation at the end of the bending stroke or by subjecting the bend zone to compression.

Spring back is influenced not only by the tensile and yield strengths of the sheet material, but also by its thickness, as well as the bend radius, bend angle, and the ratio between the bending radius and sheet metal thickness. Spring back occurs with all types of forming by bending [Schuler, 1998].

## CHAPTER 3

### METHODOLOGY

#### 3.1 Introduction

The methodology used for this research was as follows: First blanking, deep drawing and bending processes were modelled and simulated independently using FEA and thereafter verified experimentally. Following onto this, a full process analysis of the coupled process with subsequent experimental verification was undertaken. All the workpieces used in the experimental work here were cut from the same sheet. As for the full process, the same workpiece was used for all the three processes. Optimisation of the coupled processes simulated in this work was done by varying the parameters in the simulation constrain equation.

#### 3.2 Computer Models and FEA Simulations of Forming Processes

In this study, both the sheet-metal and the dies were modeled in three dimensions. The modeling was done in SolidWorks 2005 and the analysis in Cosmosworks 2005. The tooling used in all the three processes was modeled as rigid bodies. In all simulations for the sheet-metal, the model type used was von Mises failure criterion with a non-linear analysis, solid mesh and direct sparse as a solver. The Newton Raphson method was used as an iterative solver in all cases.

The von Mises criterion was chosen because it is the best model for describing yielding since it combines the stresses developed during deformation into an equivalent stress which is then compared to the yield stress of the material. [Shigley, 1976]. The usual form of the Von Mises criterion is

$$2\sigma_0^2 = (\sigma_1 - \sigma_2)^2 + (\sigma_2 - \sigma_3)^2 + (\sigma_3 - \sigma_1)^2 \dots\dots\dots \text{Equation 3}$$

where  $\sigma_0$  = equivalent stress and  $\sigma_1, \sigma_2, \sigma_3$  = principal stresses.

The non-linear analysis was chosen because, in all sheet metal forming processes, there is contact between workpiece and the forming tools. Contact is a common source of nonlinearity because of the boundary conditions that change when loading. Non-linear analysis has control on each load and restraint individually by a time curve [Cosmosworks Manual, 2005]. The Newton-Raphson was used as an iteration method because it has a high convergence rate and its rate of convergence is quadratic. The Direct Sparse solver has more chances of convergence for highly nonlinear problems.

In each simulation, a Coulomb friction coefficient value of 0.1 was used to describe the interface friction condition between the tooling and sheet-blank. The contact between the sheet and tool was assumed to be uniform. The material properties of AISI 1023 carbon steel were used for the finite element simulations. Table 3.1 shows the mechanical properties of the AISI 1023 mild steel sheet used in all the three simulations.

**Table 3.1: Mechanical Properties of AISI 1023 Carbon Steel (Cosmosworks Manual, 2005)**

Properties	Value
Young's Modulus, E	$2.05 \times 10^{11}$ N/m <sup>2</sup>
Poisson's ratio,	0.29
Initial Yield stress	282 Mpa
Ultimate Tensile Stress	420 Mpa
Shear strength	350 MPa
Density	7858 kg/m <sup>3</sup>
Strain hardening factor	0.85

### **3.2.1 Input Data for Simulations**

In the 3D models that were generated using SolidWorks and which were analysed in Cosmosworks, the required material data were obtained from the Cosmosworks library which included the following:

- Young's modulus
- Specific mass density
- Poisson's ratio
- Coefficient of friction
- Parameters for strain hardening curve for AISI 1023 carbon steel.

### **3.2.2 Simulation Procedure**

The simulation models created accounted for the different tool components, data for the material and process parameters such as binder force and punch velocity. The simulations basically involved the following steps:

- Assembling the models created in Solidworks
- Defining the process parameters.
- Meshing and generating results
- Post- processing results using Excel after importing them from Cosmosworks

A design table for each model of the forming process was then created. The design tables work as a product configuration. Using the design table, the modelled assembly was then adjusted to a desired configuration. Once the data was input into the design tables and the assembly updated to conform to the desired configuration, optimal design parameters for the forming process were obtained.

### 3.2.3 Meshing

After the creation of a geometric model, Cosmosworks program automatically subdivides the model into small pieces of simple shapes (elements) connected at common points (nodes). Mesh sizing or re-meshing as required was thereafter achieved automatically with the help of the mesh control function of the software.

This automatic mesher was used to generate a mesh based on a global element size, tolerance and local mesh control specifications.

In the early stages of design analysis where approximate results were required for initial analysis, a larger element size was specified for a faster solution. For a more accurate solution, a smaller element size was used. A compromise between mesh size and computer processing time was made during remeshing process.

### 3.3 Modelling of the Blanking Process

The blanking process was modelled as shown in Figure 3.1. Due to the axial symmetry of the model, it was not necessary to model it all through 360 degrees and a choice of 45 degrees sector of the sheet metal was chosen for simulation to reduce on computing time. The geometrical properties of the blank used are shown in Table 3.2. An initial condition of surface contact between the tool and the metal sheet was assumed.

**Table 3.2: Geometrical Properties of the Blanking Process**

Parameter	Size (mm)
Punch radius	60.5
Die radius	60.65
Punch cutting edge radius	0.15
Die punch clearance	0.05

The die arrangement of the blanking process is similar to that of the deep drawing processes except that in blanking the binder pressure is set high enough not to allow any relative movement between the blank and the die. The die/punch clearance in blanking is also set lower than that of the deep drawing process. This is to allow the shearing action to occur as the punch moves relative to the die.

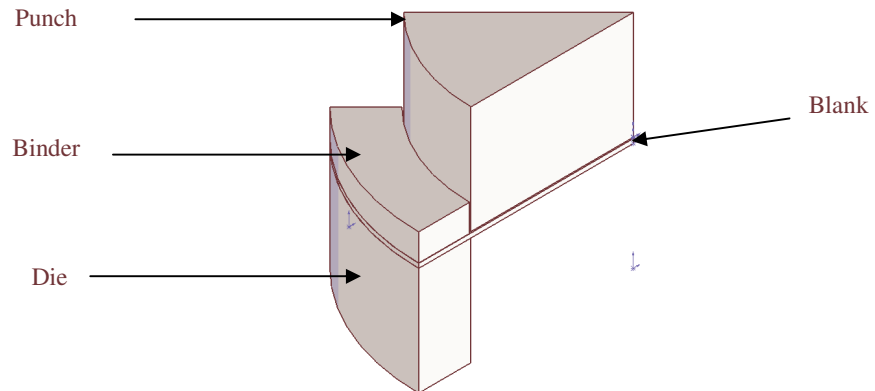


Figure 3.1: Finite Element Model of a Blanking Process

During the blanking process, an upper blade (punch) and a lower blade (die) are forced past each other with the space between them (clearance) determined by a required offset. In blanking, the die is always kept stationary as the punch is lowered.

The theoretical blanking force can be calculated from the empirical formula (Equation 4). The force  $F$  is equal to the area to be sheared  $A_s$  times the shearing strength  $\tau_s$  for the material. Mathematically [Sharma, 2003],

$$F = k\tau_s A_s \dots\dots\dots \text{Equation 4}$$

where  $k$  = factor that takes into account the work hardening of the material during deformation, material non-homogeneity, non uniformity of the sheet metal, amount of clearance between the punch and die, and the state of the cutting edge. The factor is determined experimentally by measuring the punch force for different values of sheet thickness and the shear length.

### **3.3.1 Blanking Simulation Procedure**

After the models were produced, they were assembled within SolidWorks. Thereafter, for analysis the assembled models were exported to Cosmosworks. In the modeled assembly, the die was restrained in all three axes of a three dimensional space in order to ensure it is completely immovable. The top face of the punch was also restrained in the two axes (horizontally) and allowed a displacement of 3mm in the vertical plane. The binder was made immovable with no translation to ensure that the workpiece does not slide between the die and the binder.

All the side faces of the punch, binder, blank and the die were symmetrically restrained allowing only one eighth of the blank to be modelled. A standard mesher of solid type of elements, with a total number of 3356 elements was used. The element size used was 6.5632 mm with a tolerance of 0.32816 mm. A surface contact element was used between the punch and the blank while bonded contact elements were used for the binder-blank and blank-die contact. Workpiece separation and distortion during the blanking process was predicted by comparing the simulated and experimental results based on a study of the critical areas of the workpiece. The stress-strain that developed in the workpiece was thereafter compared with real tensile values. If the value of the simulated maximum plastic strain was higher than the real fracture plastic strain, this was taken to imply that sheet metal workpiece under study would break. If it was lower, then this signified that the blank would not break away or separate. Therefore, depending on the plastic strain and stress evolution during simulation, it was possible to predict what would happen to the workpiece under the imposed loading.

### **3.4 Deep Drawing Simulation**

Deep drawing process is characterized by a large number of process parameters and their interdependence. These are material properties, machine parameters such as tool and die geometry, workpiece geometry and working

conditions. Table 3.3 shows the process parameters used during the deep drawing simulation.

**Table 3.3: Tool and Process Parameters for a Deep Drawing Simulation**

1	<b>Punch</b>	
	Diameter	59.4 mm
	Nose radius	3
2	<b>Draw Die</b>	
	Die Profile radius	4 mm
	Die Diameter	60.8 mm
3	<b>Blank Holder</b>	
	Inside diameter	62 mm
	Outside Diameter	100 mm
4	<b>Blank</b>	
	Thickness	1.2 mm
	Diameter	100 mm
5	<b>Process Parameters</b>	
	Blank Holder pressure	0.825 MPa
	Friction	0.1

### 3.4.1 Modelling of a Deep Drawing Process

A three-dimensional deep drawing process was modelled as shown in Figure 3.2. Similarly, due to symmetry only a 45 degrees sector of the model was analysed. The die bottom face was restrained both in rotation and translation motion and was set at zero. The binder provided the necessary pressure required to prevent wrinkling and was restrained to a downwards motion only. The top face of the punch was with respect to reference geometry Top Plane given a displacement -50 mm normal to the reference plane.

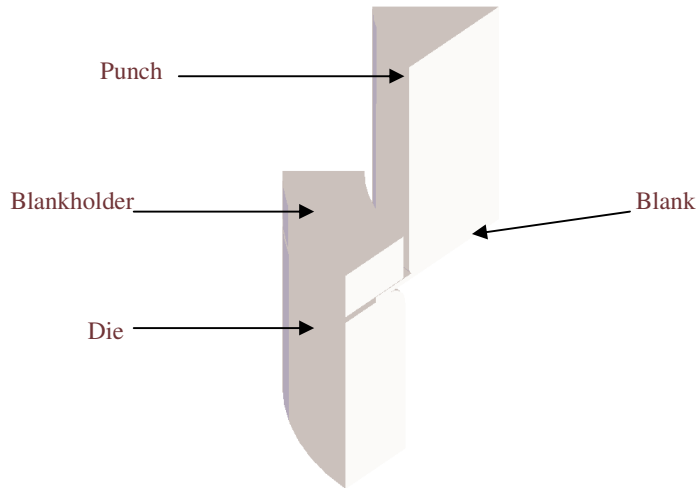


Figure 3.2: Deep Drawing Solid Model

In the deep drawing simulation, a total number of 7401 elements were used with an element size of 3.6376 mm and a tolerance of 0.18188 mm. A large deformation elasto-plastic material model was used which comprises an elastic and plastic part.

### 3.4.2 Deep Drawing Simulation Procedure

The drawing force can be determined by the empirical formula [Sharma, 2003]:

$$F = A_s \sigma_y \left( \frac{D}{d} - C \right) \dots \dots \dots \text{Equation 5}$$

where  $D$ = blank diameter,  $d$  = shell diameter,  $\sigma_y$  = yield stress of the material and  $c = 0.6$  . The drawing ratio  $D/d$  takes into account the relation between the blank and the shell diameters. The drawing ratio depends on factors such as type of material and amount of friction present. The usual range of the maximum drawing ratio for mild steel is 1.6 to 2.3. The constant  $C$  accounts for friction and bending effects and ranges from 0.6 to 0.7 [Sharma, 2003].

### 3.5 Modelling of a Bending Process

The bending simulation investigated was edge bending which is frequently performed on deep drawn parts. The geometric properties used in the bending simulation are shown in Table 3.4.

**Table 3.4: Geometrical Properties of the Bending Test**

Parameter	Size (mm)
Punch radius	1
Die radius	0.5
Punch cutting edge radius	0.5
Bend length	50
Bend Angle	90 <sup>0</sup>

A 90<sup>0</sup> edge bend simulation model is shown in Figure 3.3. The blank was held firmly on the sides to prevent its movement during bending. The blank is held down by a pressure die before the punch contacts it. A clearance equal to the plate thickness was provided for between the punch and the pressure die.

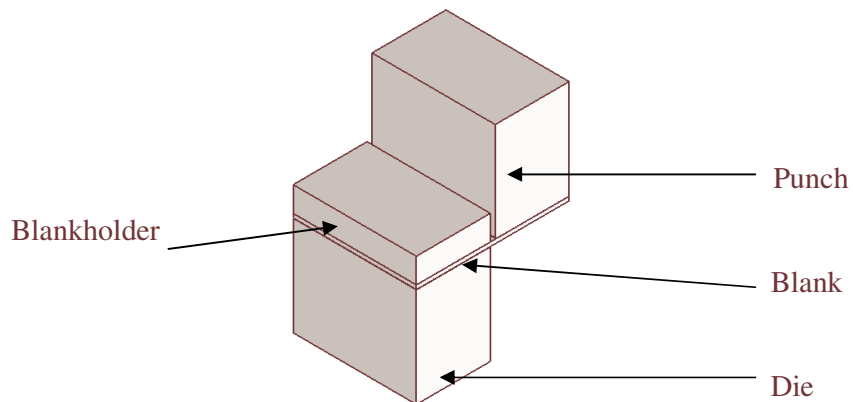


Figure 3.3: Edge Bending Simulation Model

### 3.5.1 Bending Process Simulation Procedure

The bending force depends on the stock thickness ( $t$ ), the length of the bend ( $l$ ), the width of the die opening ( $w$ ) and type of bend. For edge bending the force required is given by [Sharma, 2003],

$$F = K \cdot \frac{l \cdot t^2 \cdot \sigma_{ut}}{w} \dots\dots\dots \text{Equation 6}$$

Where  $\sigma_{ut}$ ,= ultimate tensile stress of the material and  $K$  = die opening factor. The die opening factor,  $K$ , varies from 1.2 for a die opening of 16t to 1.33 for a die opening of 8t. The magnitude of the bending force is directly proportional to the length of bend,  $l$ , and the thickness,  $t$ . The bending force is inversely proportional to the width of the die opening.

### 3.6 Optimisation Procedure

The optimisation procedures developed in this study was based on the knowledge of underlying sheet-metal forming mechanics and were validated by experimental results.

#### 3.6.1 Deep Drawing Optimisation Procedure

The optimization scheme for optimizing the geometry of the cup was developed with the aim of optimizing the minimum drawing force required. The optimization modeling procedure was developed from Equation 3 which shows the force needed to draw a shell and is equal to the product of the cross sectional area and the yield strength in tension of the work material.

Mathematically the forming load can be expressed as:

Minimize  $F(x) \geq 0$

To satisfy the following constraints

$$l_i \leq x_i \leq u_i \quad i = 1, \dots, n.$$

Where  $F(x)$  is the objective formability function and  $x$  represents the design variables and  $l_i$  and  $u_i$  are the lower and upper bound on the  $i$  th design variables respectively.

The optimization variables used in this case were

$$0.6 \leq C \leq 0.7; \quad \text{and}$$
$$1.6 \leq \frac{D}{d} \leq 2.3$$

The combination of the values for  $C$  and  $D/d$  used in the optimization scheme were

Lower value = 0.6 and 1.6

Upper value= 0.7 and 2.3

The variables used were taken from the maximum and minimum values from drawing ratio, friction and bending constants.

### 3.6.2 Objective Formability Function.

The aim of an optimization is to improve the quality and reliability of the forming process. This was achieved by first defining an objective cost function that reflects the forming process. The design variables in the objective function are of two types:

1. Process parameters which are the binder force; and
2. Geometry parameters which are profile parameters of the die surface

The tool parameters such as radius of the die, punch radius and process parameters such as blank holder and coefficient of friction were optimized using

the optimization scheme with respect to material properties and working conditions. The value of the objective function reflects the quality of the single forming process predicted by sheet metal forming simulations. A higher value of the objective function indicates worse formability; a lower value indicates better formability.

The criteria used to decide whether a forming process was practical and reliable were as follows:

- No cracks should occur
- The thinning should not exceed a given value
- Minimum stretching
- No wrinkles.

All the above four criteria were evaluated based on the strains (major strain =  $\epsilon_1$ , minor strain =  $\epsilon_2$ ) at the end of the forming process. The criteria were evaluated with the help of the Forming Limit Diagram FLD. The integration points of the finite element mesh ( $\epsilon_1, \epsilon_2$ ) were plotted on the FLD. The points which were above the Forming Limit Curve (FLC) denoted a high risk of cracking, thinning, stretching and wrinkling. Finally, when all four criteria were added, an optimized process was obtained.

### **3.6.3 Forming Limit Diagram (FLD)**

Forming limits of sheet metals are influenced by several physical factors of which the most important ones are material work-hardening, strain rate sensitivity, plastic anisotropy, the development of structural damage, in-plane and out-of-plane deformation and strain path. A number of different theoretical approaches have been proposed to explain the localized necks in biaxial tensile fields. Up to now, there have been two broad theoretical frameworks to explain necking in biaxial tensile fields.

Figure 3.4 shows that when there is insufficient stretching, the sheet metal has a tendency to form wrinkles. Similarly if the material is loaded excessively, the

risk of cracks developing are very high. Therefore a compromise has to be struck so that the forming processes are within the safe region.



Figure 3.4: Diagrammatic Representation of the Assessment of the Various Regions of Forming Deformation [Arwidson, 2005].

The concept of the Forming Limit Diagram (FLD) has proved to be very useful for representing conditions for the onset of sheet necking [Gandhi et al. 2005], and is now a standard tool for characterizing materials in terms of their overall forming behaviour. The studies conducted on the analysis of sheet metal formability are too broad and therefore this study will be restricted to the analysis of metal formability using Forming Limit Diagrams (FLDs), and the theories advanced toward the understanding and predicting strains under complex loading conditions.

The development of the production of new sheet metal parts requires a set-up of forming operation or several progressive operations and demands a good knowledge of the attainable forming limits of the material. It is understood that above the forming limits localized necking and fracture occurs. It is possible to perform the analysis of the forming process in a digital environment when fracture data and the material forming characteristics are known as input parameters. Sheet metal forming evaluation with a FLD based on comparison of the first main strain ( $\epsilon_1$ ) versus the second strain ( $\epsilon_2$ ).

Forming Limit Diagrams (FLDs) offer a convenient and useful tool in the analysis of the sheet products manufacturing processes. They help identify critical combinations of major strains ( $\epsilon_1$ ) and minor strains ( $\epsilon_2$ ) on the sheet surface at the onset of necking or failure. With a FLD it is possible to evaluate

different strain conditions on the same diagram and determine fracture limits for a particular strain combination.

The strain-based forming limit criterion of FLDs is widely used throughout the sheet-metal forming industry to gauge the stability of the deformed material with respect to the development of a localized neck prior to fracture. Strains below the FLD curves are acceptable while those above the curves signify the occurrence of local necking and are therefore not accepted. (see Figure 3.5 for details.)

In many sheet-metal forming operations, deformation is predominantly in the form of stretching. When a sheet is progressively thinned, two modes of plastic instability are possible, that is diffuse and localized necking. Diffuse plastic instability occurs when the extension is larger than the sheet thickness.

Many of these characteristic can be conveniently assessed by a formability plot, where the major and minor strains predicted by the simulation are compared to the specific FLD for the material to identify potential problems. Generally, the safe region for forming processes can be assessed as shown in Figure 3.5. The curve that forms the lower boundary of the area *C* is the forming limit curve. The curve describes the level of strain that the actual material can withstand before fracture, cracking or wrinkling commences. Following a rule of thumb, experience has shown that the component being formed will not break if the strain level in it does not exceed 80% of the level of the forming limit curve [Meinders, 1998].

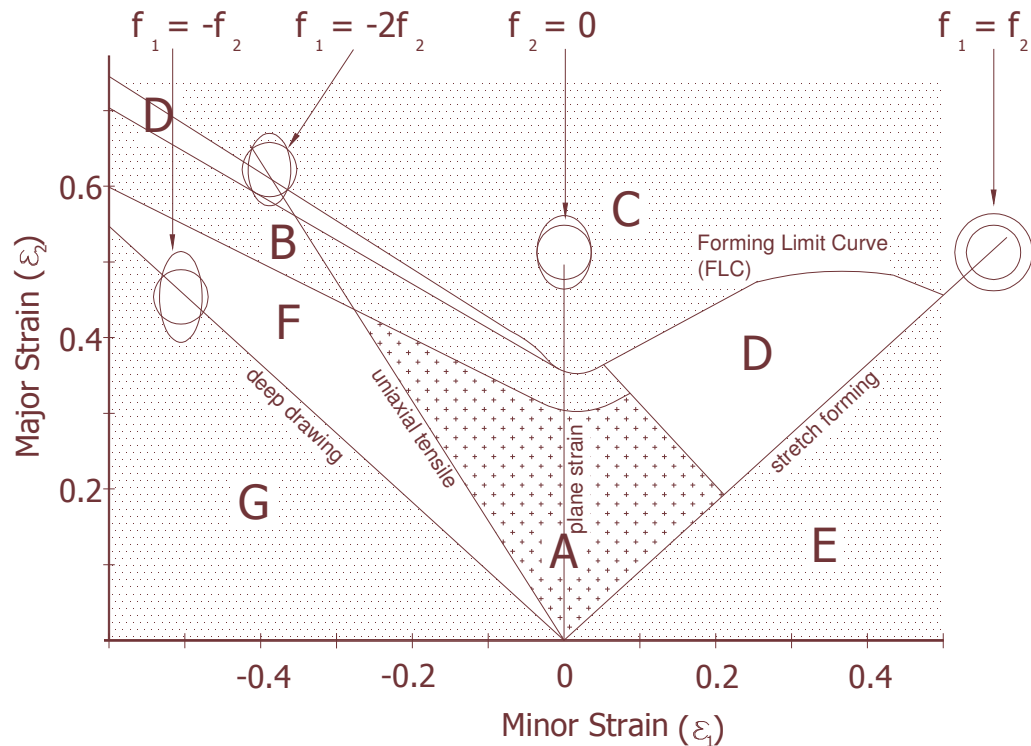


Figure 3.5: Typical Forming Limit Diagram [Arwidson, 2005]

The different areas in the forming limit curve shown in Figure 3.5 are:

- A. The recommended region for forming processes
- B. Danger of rupture or cracking.
- C. The material has cracked
- D. Severe thinning
- E. Insufficient plastic strain, risk of spring back.
- F. Tendency to wrinkling
- G. Fully developed wrinkles

In sheet metal forming processes, the engineer is usually most interested in sheet forming characteristic of the part including:

- The presence of wrinkles
- High tensile strains leading to cracks

- Low ductility resulting in 'loose' material and poor surface finish.
- Skid lines where the sheet is marked by localised punch contact.
- Minimum blank outline to ensure sufficient material is available.

### **3.7 Experimental Verification**

Experimental blanking, deep drawing and bending processes were all done on a Vremac Hydraulic Press shown in Figure 3.6. The press has sensors which automatically pick information via the Angela (computer) System immediately the ram is set in motion. For each experiment, a trial run was carried out and data collected before the final data collection run.

During experimentation, the conditions of the setup were kept as close as possible to depict the simulation conditions, thus for instance, the dies and workpiece sizes that were used in both the experiment and simulation were the same.

#### **3.7.1 The Vremac Hydraulic Press**

All the three experiments were done on a Vremac Hydraulic Press fitted with a data capturing system called the Angela System. Three different die sets were used for the blanking, deep drawing and bending processes. Castrol HP 90 oil was used for lubrication in all processes.

For taking measurements during experimental setup, protractor, steel rule and calipers were used. The mounting of the dies on the machine vice was manually done with a spanner.

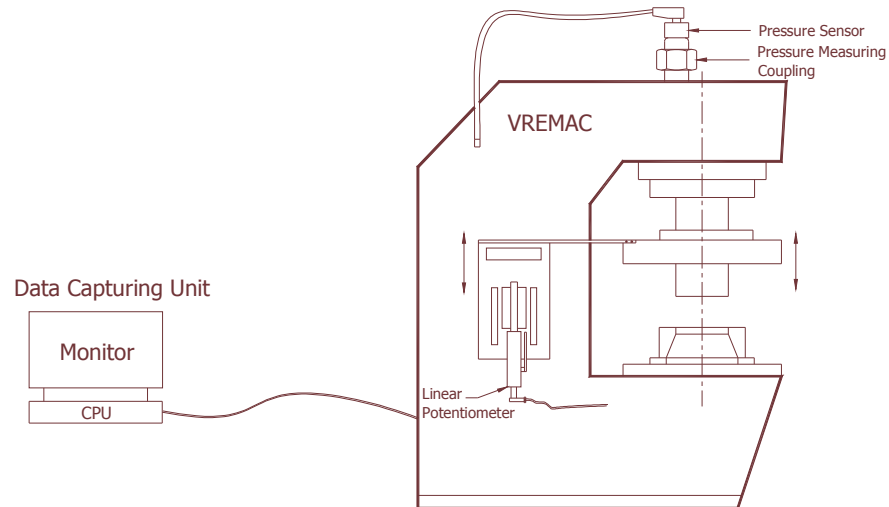


Figure 3.6: The Vremac Hydraulic Press

### 3.7.2 Experimental Procedure

The die was first mounted on to the bottom die shoe and the punch onto the top die shoe. The top die shoe together with the punch mounted onto the holder, were then firmly fitted onto the press. With the die directly below the punch, the ram was lowered until it met with the die. A strip of 1.6mm (same size as the blank) was used to set the clearance for the material. Thereafter, the bottom die shoe was securely fixed to the press bed. This was set as a lower limit.

With the linear potentiometer meter fixed to the press, the punch was moved 125mm clear of the die and a blank inserted and lubricated over the die opening. The press upper limit was set by pulling the linear potential meter shaft to wedge into the rubber carrier.

When running the experiments, starting of the Angela system and the commencement of the downward motion of the punch were done simultaneously. Once the punch penetrated the workpiece it was withdrawn immediately. All the processes took 12 milliseconds.

### **3.7.3 Deep Drawing Process Experiments**

The experimental set up was typically the same as for the other processes. The deep drawing forming operation was undertaken on a cylindrical shaped component with same dimensions the as those used in the deep drawing simulation.

The tool set up had a fixed die with a punch moving vertically downwards and the blank holder applying a force onto the blank which in turn was supported by a fixed die. The initial height between the punch and the blank was set at 50mm above the workpiece. The blank and tools were lubricated with standard oil for sheet metal forming processes.

### **3.8 Coupling Simulations**

If several operations are executed on a single workpiece, steps must be taken to ensure that sufficient material flow is available to replace the material displaced during the preceding forming process. Otherwise, under certain circumstances, it is possible that significant weakening or fracturing could take place on the sheet metal workpiece. In addition, the force required to achieve the final shape increases due to the work hardening of the material [Schuler, 1998].

Mild steel has relatively higher stretch distribution characteristics, making it more stretchable and drawable than conventional high strength steels. Stretch distribution characteristics determine the ability of steel to stretch over a large surface area.

The better the stretch distribution, the more the steel can stretch over the draw punch to create the final geometry. Stretch distribution affects not only stretchability, but also elastic recovery, or springback, and the metal total elongation. [Kobayashi et al. 1989].

In a sheet metal forming production line it is necessary to perform a long virtual simulation chain before prototyping and testing. This simulation includes

different forming analysis of displacements, stress and strain with Finite Element Analysis tools. The important points of interest on a blank are those that undergo multiple forming processes and the damage distributions. These form the basis for deciding if and how the redesign of the product is performed.

Therefore, by using strain distribution results from simulation results of different processes and plotting them on the same Forming Limit Diagram (FLD), it is possible to quantify the influence of each process on the blank. In this study, plotting the strains of different simulations on the same FLD was used as a basis for coupling or linking simulations.

## CHAPTER 4

### RESULTS

#### 4.1 Introduction

This chapter presents the results of blanking, bending and deep drawing simulations as well as experimental results from each of these forming processes. The experimental results were used to verify the accuracy of the process models used in the simulations. The full deep drawing process consisting of the three forming processes is represented in Forming Limit Diagrams (FLD) in which forming limit strains are indicated.

The two most important items in the analysis of metal forming process are the determination of forming loads and the extent of deformation to which a workpiece can be subjected before it fails. Process simulations generated stress and strain contours. Strain contours were used to assess the forming limit by checking the onset of localized necking over all possible combinations of strains in the plane of the sheet. This was used to determine formability for the whole process under investigation. The stress contours were used to determine the forming loads during workpiece deformation.

#### 4.2.1 Blanking Simulation Results

The contour plots shown in Figures 4.1a and b illustrate the evolution of the damage field and the propagation cracks in this field. It is evident in both plots that the stress and strain in the damage zone increases towards the shear line. The stresses in the material close to the cutting edges reach a value corresponding to the material shear strength (350MPa). The maximum strain occurred at the middle of the blank along the shear line. This was determined by comparing the colours on each of the diagrams with those on the stress or strain scales on the right of each contour plot diagram. The probing function of the simulation software, which operates to extract exact data at specific points

on a contour plot diagram, was applied to extract values of stress or strain at required points on the contour plots shown here.

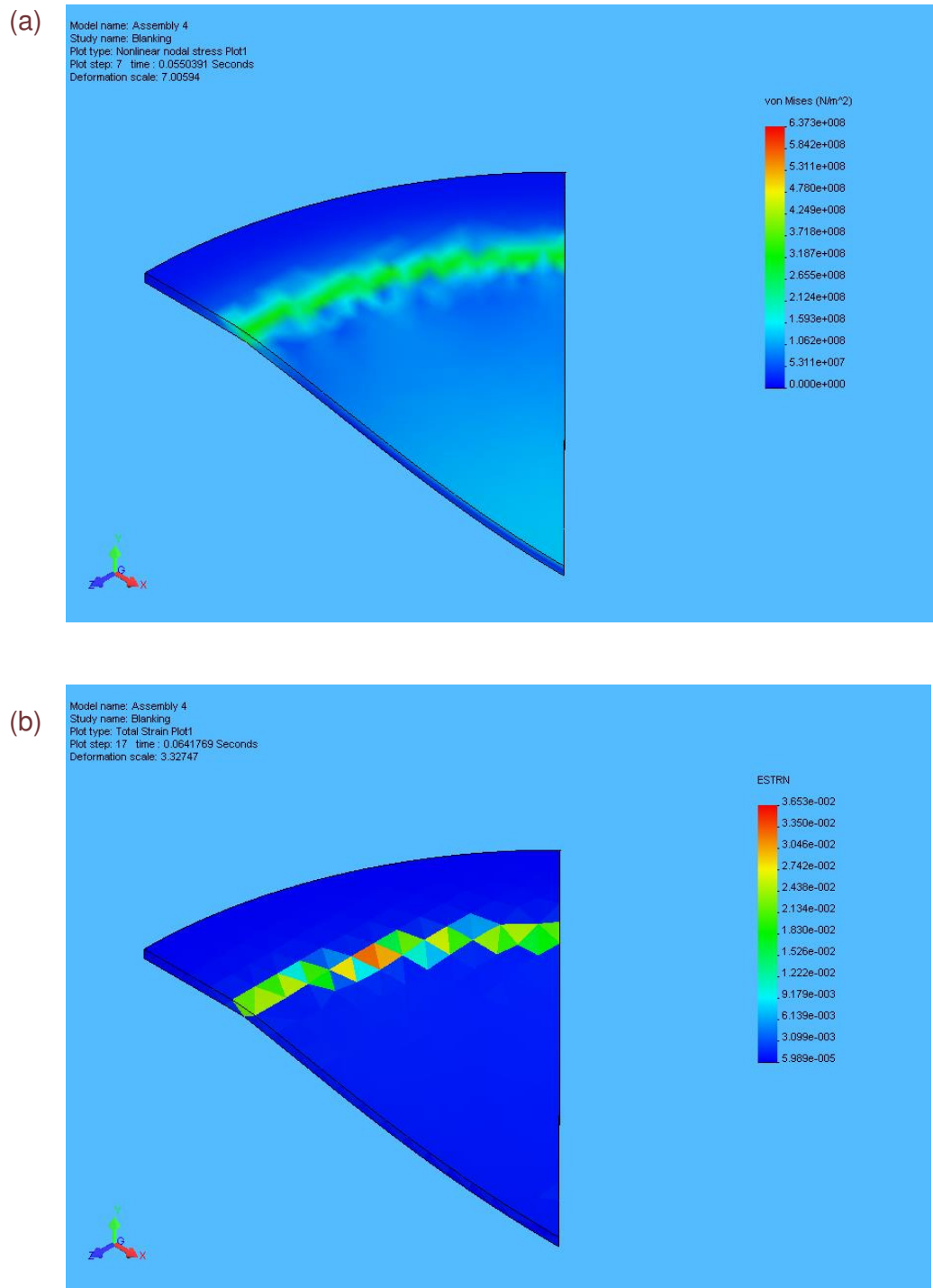


Figure 4.1: Contour Plots for a Blanking Process Showing (a) von Misses Stresses and (b) Strains

The punch force-displacement graph (Figure 4.2) generated in this simulation, shows varying forces with punch displacement. The punch was modelled with the workpiece material in contact with it and hence the graph generated shows an initial loading at the start of the simulation.

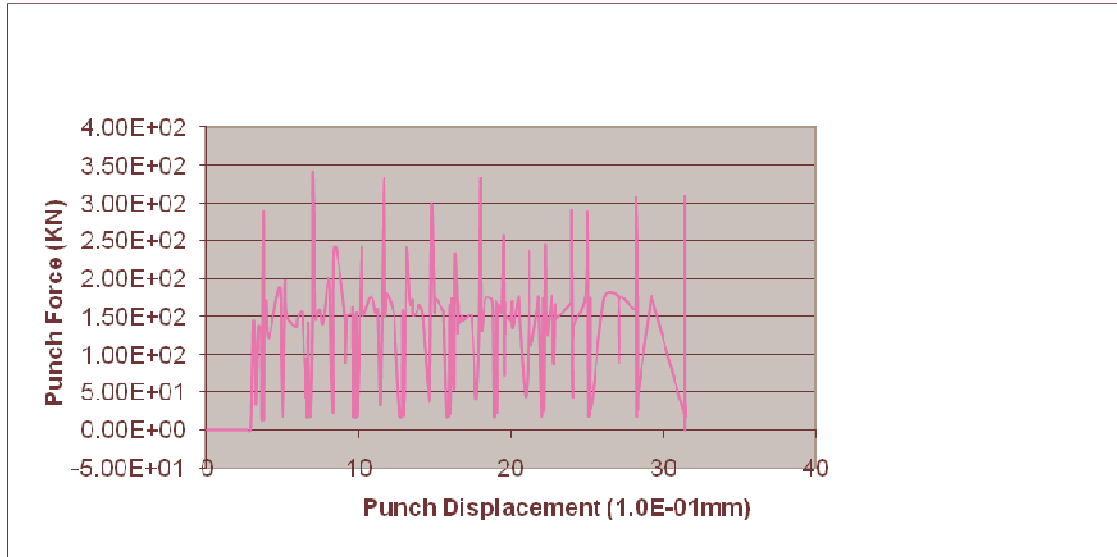


Figure 4.2: Punch Force Against Displacement for a Blanking Process

It can be deduced that punch penetration begins to occur between 0.5 and 1.2 mm of the punch displacement at which point crack initiation begins. This is because the first punch peaks occurred in this region. Beyond this region, the punch force reduced steadily as a result of plastic deformation. At this stage the material is expected to be undergoing necking. Thereafter, the subsequent rise of the peaks can be attributed to the formation of burrs.

#### 4.2.2 Bending Simulation Results

Predicting the bending strain is important in bending process design and operation. Successful bending processes require production of plastic strains so that the work pieces are permanently deformed. This strain, however, should be less than the relevant failure strain.

The von Mises contour plots presented in Figure 4.3(a) showed that around the bend area the stress level reached 300 MPa which was beyond the yield stress

of 282 MPa for the material an indication that the material underwent permanent deformation. The strain in this area was 0.079 as shown in Figure 4.3(b).

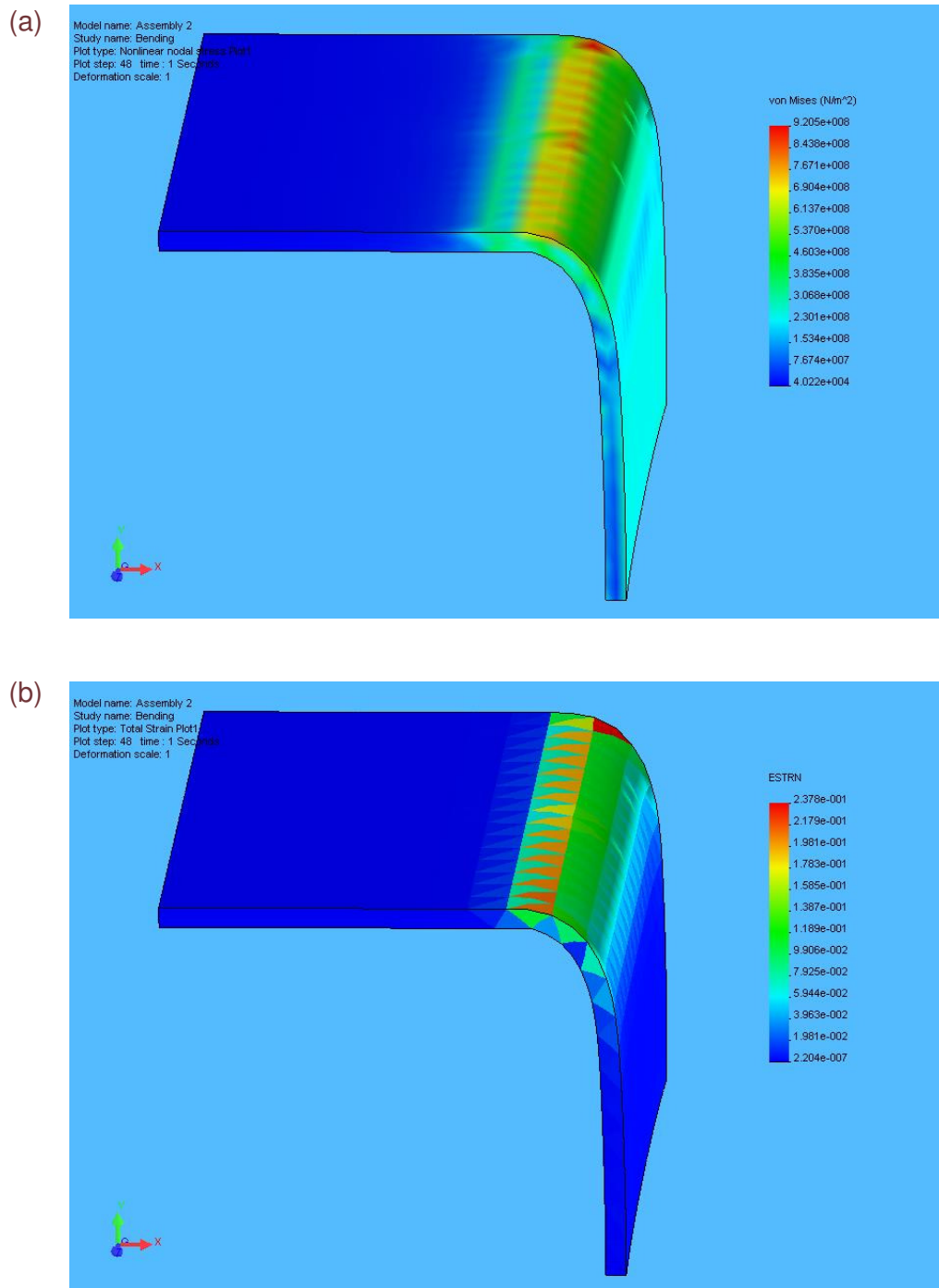


Figure 4.3a: Contour Plots of a Bending Process (a) von Mises stresses (b) Strains

Figure 4.4 shows the graph of the punch force against the punch displacement. During the bending process, the punch moved 12 mm during which the force increased steadily from 0 to a maximum value of 1.5 kN. Thereafter, as the punch progressed, the force reduced from maximum to a minimum value of 0.4 kN.

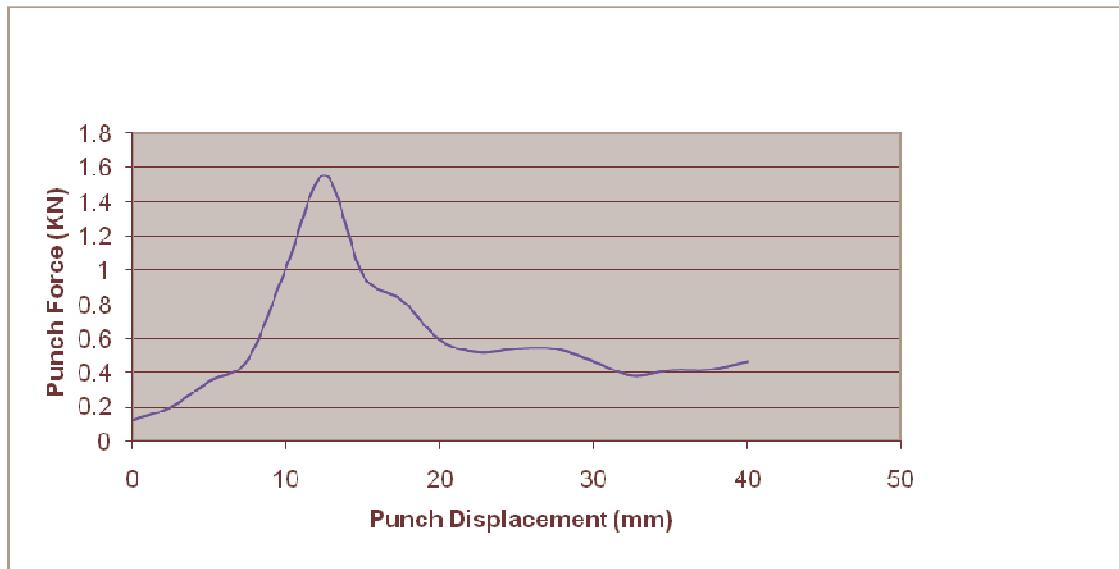


Figure 4.4: Simulated Punch Force Against Displacement for a Bending Process

### 4.2.3 Deep Drawing Simulation Results

Figure 4.5 shows the contour plot for the deep drawing process. Both the strain and stress plots show that the blank became thicker at its outer portions as it was forced into the cavity. This is normally observed in deep drawing. As the punch forces the blank into the die cavity, the blank diameter decreases and cause the blank to become thicker at its outer portions due to circumferential compressive stresses to which the material elements in the outer portion is subjected. The von Mises contour plot shows that these circumferential compressive stresses reached 360 MPa.

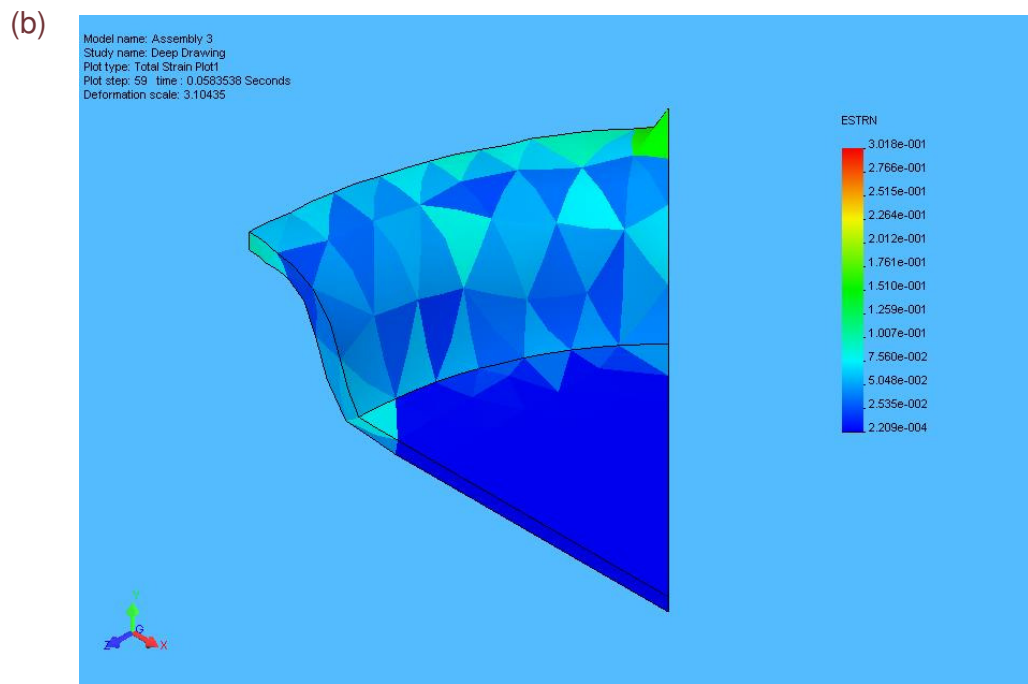
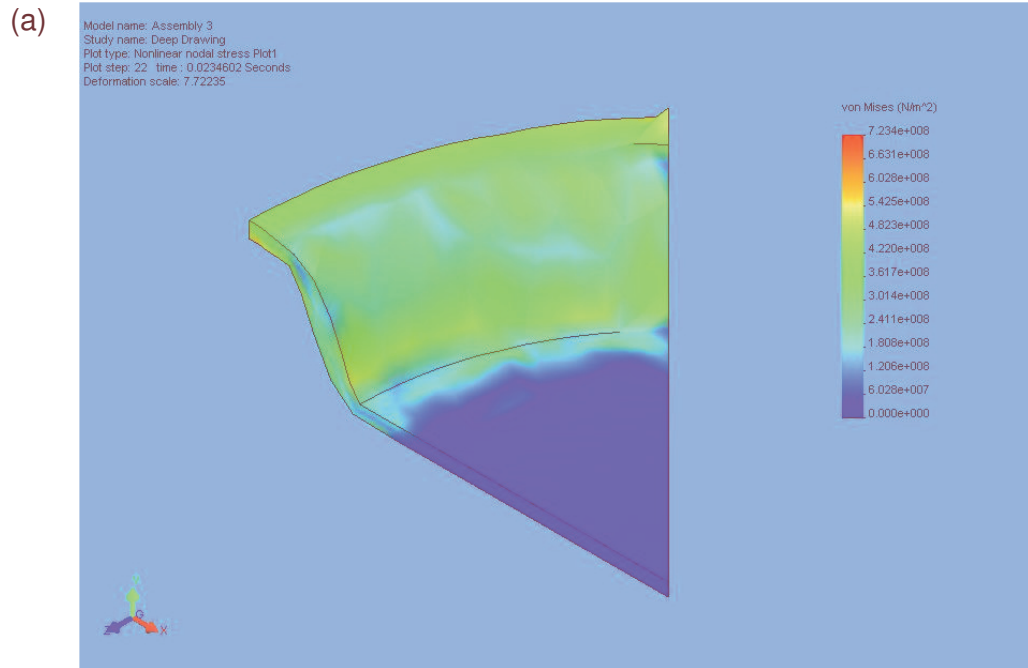


Figure 4.5: Contour Plots of a Deep Drawing Process (a) von Mises stresses (b) Strains

The contour plots shown in Figure 4.5a show a maximum Von Mises stress of 360 MPa which is below the ultimate tensile strength of 420 MPa for the blank and above the initial yield stress of 282 MPa. This confirms that forming process (deep drawing) occurred within the plastic region. It can also be seen that the portion of the blank between the die wall and the punch surface underwent some considerable tensile force and tended to stretch and become thinner. Similarly, the portion of the formed cup which wrapped around the punch radius was strained under tension in the presence of bending as shown in Figure 4.5. This portion becomes the thinnest portion of the cup and usually is the first place to fracture.

The graph of the simulated punch force against the punch displacement in the deep drawing process is shown in Figure 4.6. The deep drawing simulation done here is seen in this figure to have generated a maximum forming load of about 275 kN.

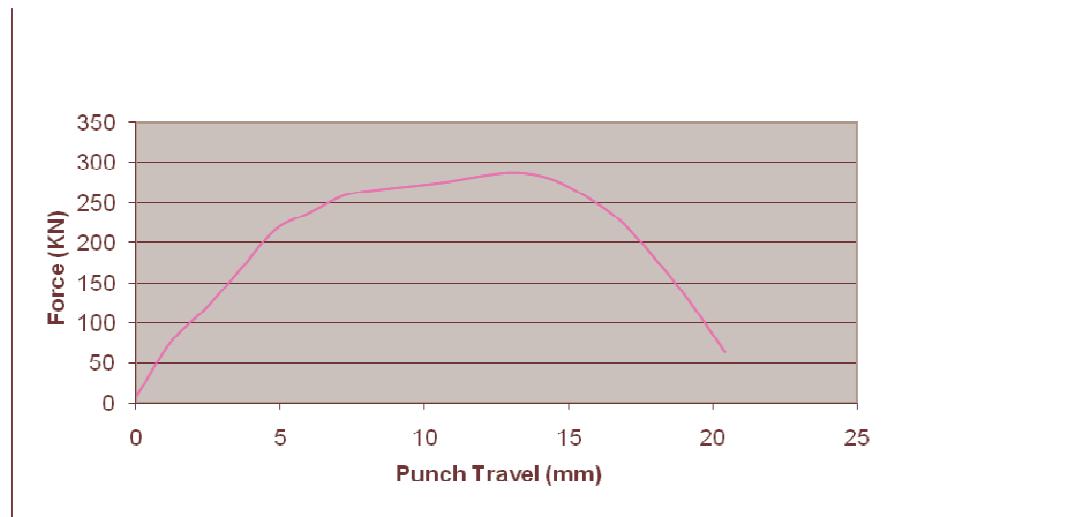


Figure 4.6: Simulated Punch Force Against Punch Displacement for a Deep Drawing Process.

### 4.3 Experimental Verification Results

In order to validate the simulations undertaken here, experimental verifications were done with forming process parameters set similar to those used in

simulation for each respective process. The stresses/pressure and displacement data generated from these experiments were used for analysis and comparison with the results from simulations.

#### 4.3.1 Blanking Process Experimental Results

The experimental blanking process was carried out with the geometrical setup and a material with the mechanical properties shown in Table 3.1. Figure 4.7 shows the graphs obtained from the blanking experiment generated from the data obtained in the process placed in Appendix 1. The two graphs of pressure against time and displacement against time were superimposed to show the pressure that was generated as the punch was moving.

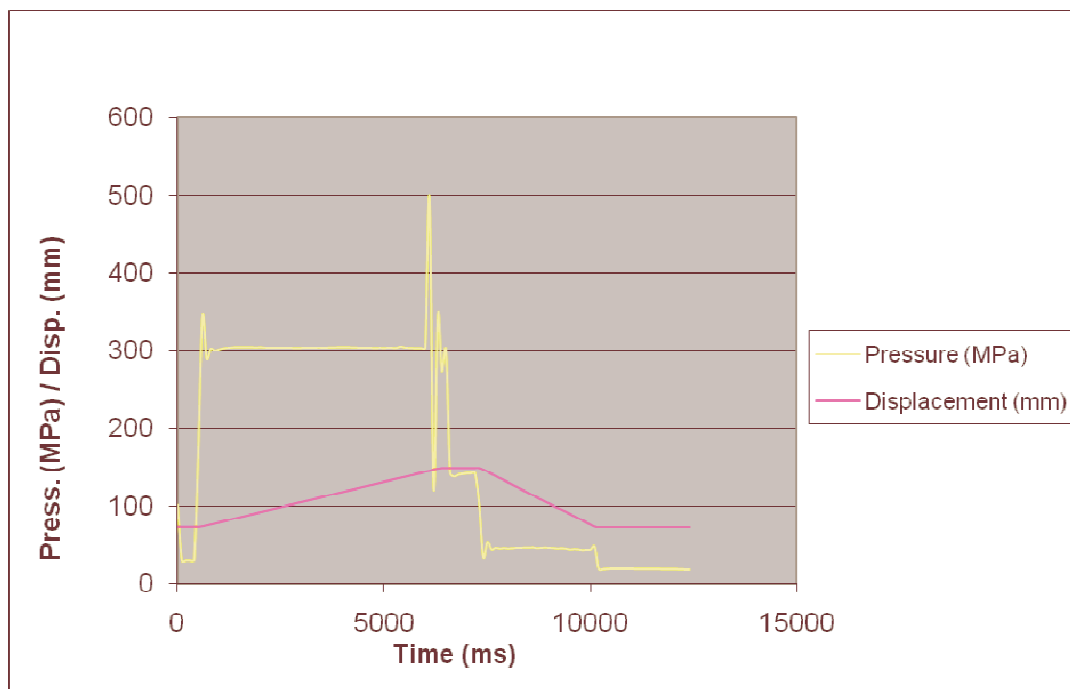


Figure 4.7: Punch Pressure/Displacement Against Time for a Blanking Process

From the graphs, it can be seen that the blanking process took between 5800 and 6200 milliseconds. The graphs also review the fact that there was an inbuilt pressure of about 300 MPa within the system before the punch touched the blank. A sudden drop and sharp rise in pressure at around 6000 ms in the two

figures confirmed the separation of the work piece before the ram was withdrawn.

The graph shown in Figure 4.7 was generated with data within an area where the deformation and separation of the blank occurred. The x-axis was confined to a punch displacement from the time the punch touched the work piece until separation in a time interval between 5600 and 6600 ms.

#### 4.3.2 Comparison of the Experimental and Simulation Blanking Results

The two graphs of the punch force versus displacement for both the simulated and experimental results were superimposed for easy comparison (see Figure 4.8). The graphs were confined within the range of the blanking process.

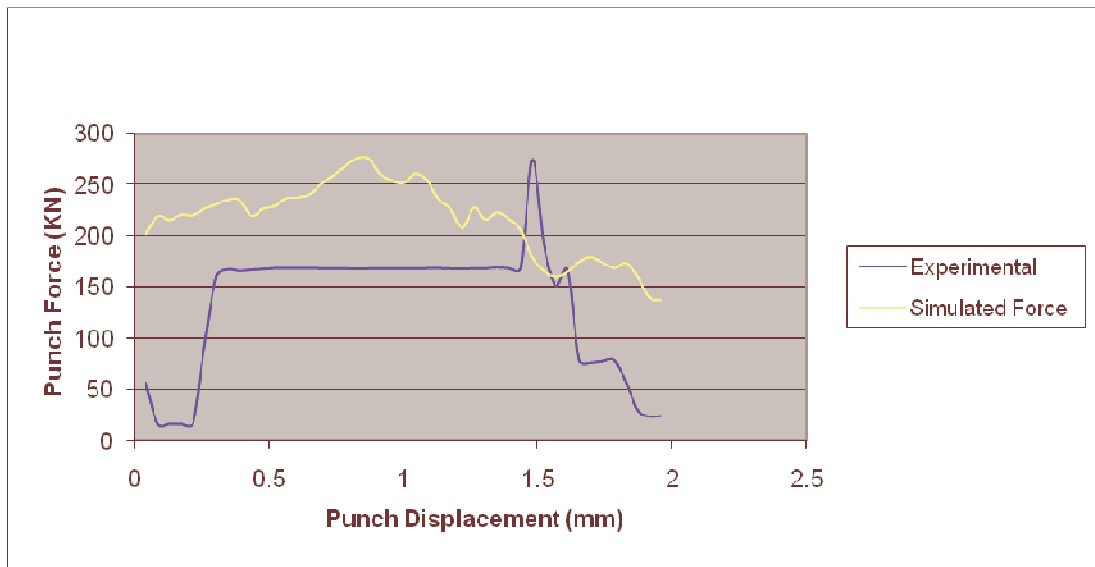


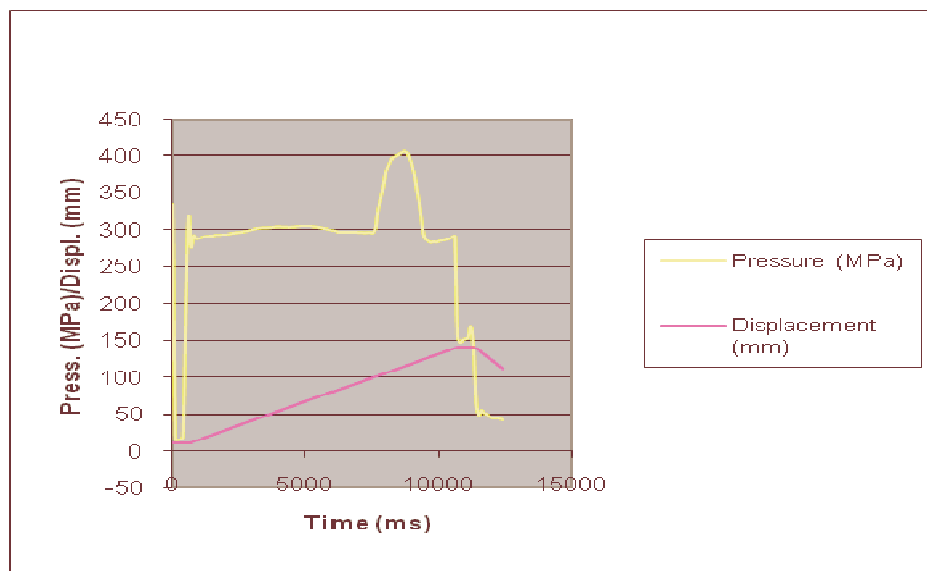
Figure 4.8: Punch Force against Punch Displacement During Blanking Process

As shown in figure 4.8, the experimental load-displacement punch curve and simulated one show some similarities. Generally, both graphs showed an increasing load at the start of the blanking process. The significant drop to 25 kN obtained in the experimental curve signified the end of the blanking process at which separation occurred. The simulated curve dropped to about 150 kN because there was no practical separation that occurred.

The simulated blanking and experimental forces both show a maximum of approximately 275 kN. However, the experimental curve obtained shows a more steep increase in force than the simulated curve because practically, blanking generally occurs within a short duration which is difficult to capture in simulations. In the simulation of the blanking simulation process, separation of the blank is predicted by the gradual reduction of the force and this requires a much wider range as compared to the experimental curve.

### 4.3.3 Deep Drawing Process Experimental Results

Figure 4.9 shows the graph generated from experimental results of a deep drawing process. The graph shows an initial in-built pressure of about 300MPa before the commencement of the deep drawing process which was estimated to have occurred between 7600ms and 9300ms.



Graph 4.9: Pressure/Displacement against Time for a Deep Drawing Process

### 4.3.4 Comparison of the Experimental and Simulation Deep Drawing Results

Figure 4.10 shows superimposed graphs of the experimental and simulated punch force against punch travel generated from the data range of 7600 and 9300 ms during which the deep drawing process was estimated to have

occurred. The graph was generated from the net pressure used in the deformation of the work piece. A maximum drawing force of 286 kN was obtained.

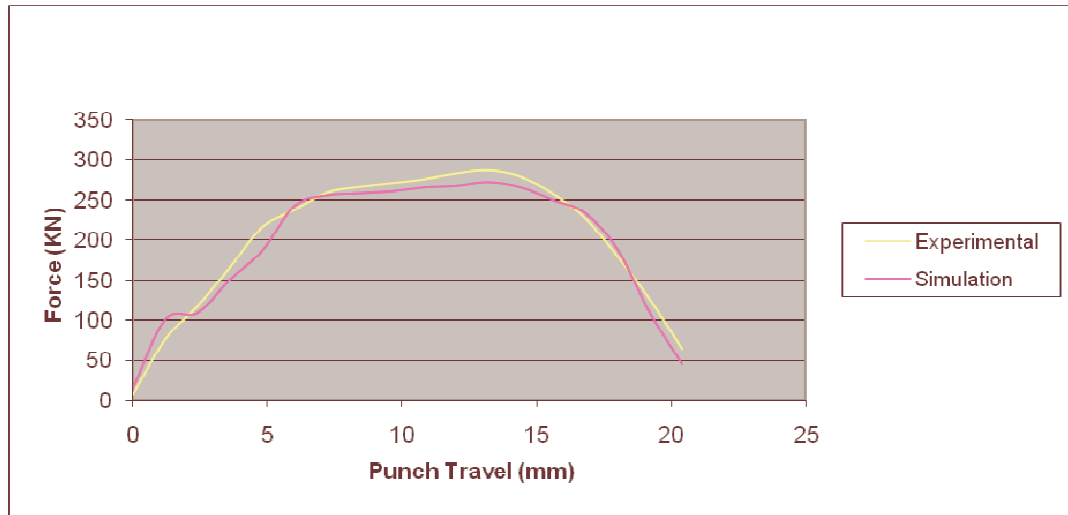


Figure 4.10: Experimental/Simulation Punch Force Against Travel for a Deep Drawing Process.

As shown in Figure 4.10, there was a rather good agreement that was observed between the simulated punch force and experimental values for the deep drawing process.

In both cases, the force steadily increased as the punch started penetrating the blank. The non-uniformity of the curve can be attributed to the impact between the punch and blank and work hardening of the material causing a non-stable forming process.

#### 4.3.5 The Bending Process

The experimental setup of the bending process was the same as that for the other two processes. The major difference between it and the other two processes was the rectangular blank shape and the die set profiles. The bend angle was set at  $90^{\circ}$  with some allowance for springback.

### 4.3.6 Experimental Results of the Bending Process

The graph shown in Figure 4.11 was generated by superimposing the experimental values of pressure and displacement against time. From Figure 4.11 it can be deduced that bending occurred during the time just before a constant displacement was recorded. The bending process ended between 7000 and 8000 milliseconds, interval at which the punch displacement was constant. From this point, the graph shows a decrease in displacement an indication of punch withdrawal.

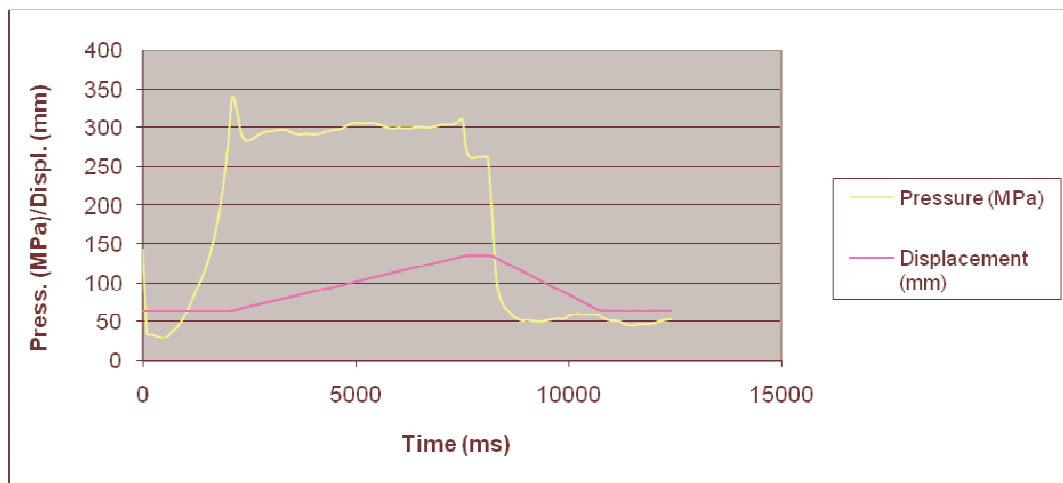


Figure 4.11: Punch Pressure/Travel against Time for a Bending Process

It is evident from the graph in Figure 4.11 that there was a pressure rise to the level of 300MPa in the system before the punch touched the blank. Therefore, to obtain the actual pressure used in the bending process a graph with a data range around the bending interval with pressure reduced by the initial 300MPa was generated and is presented here as Figure 4.12.

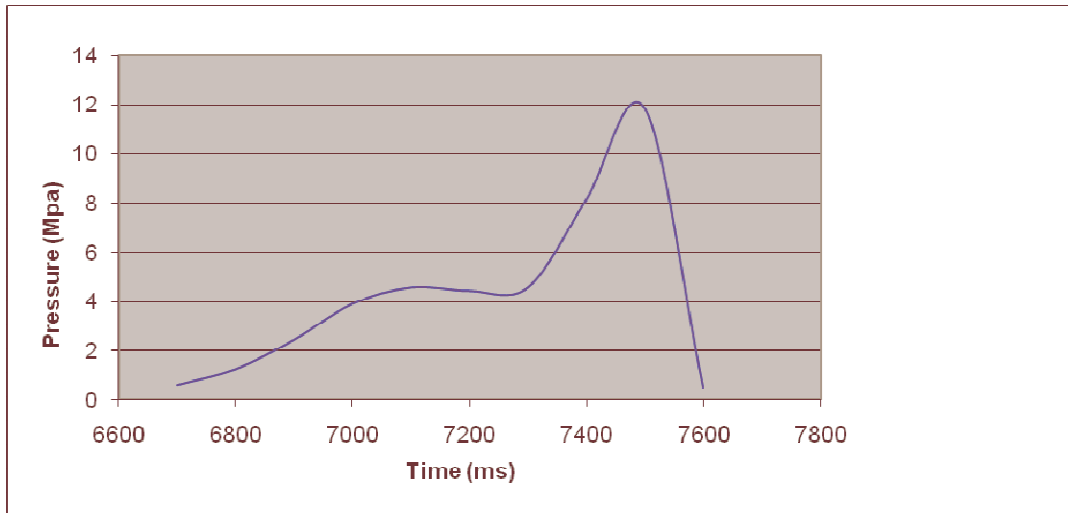


Figure 4.12: Bending Punch Pressure against Time

#### 4.3.7 Comparison of the Experimental and Simulation Bending Results

The simulation and experimental results of the bending process were superimposed to generate Figure 4.13. This was done to enable easy comparison with the related simulated result. The maximum drawing force obtained experimentally was 1.9kN.

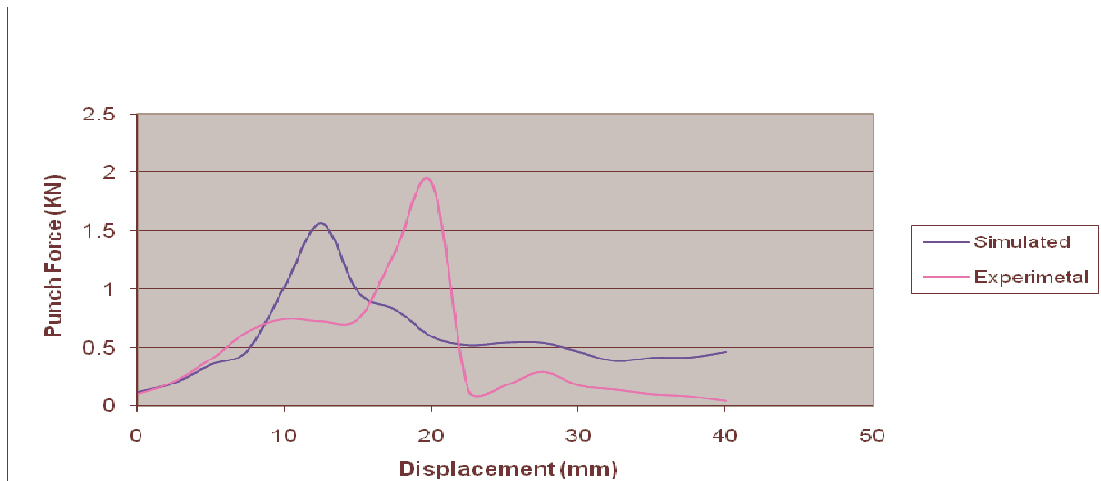


Figure 4.13: Experimental/Simulation Punch Force against Displacement for a Bending Process.

The graphs in Figure 4.13 compare well despite a horizontal displacement of their peak values of about 10 mm and a difference of the peak value of 0.5 kN

which is also evident though with reversal of the difference for the higher displacements in the graphs.

#### **4.4 The Full Forming Process**

During the full process experimentation, the same workpiece was made to undergo deep drawing, bending and blanking continuously in this order. Deep drawing was done first, and then a piece cut from the drawn cup for the bending and blanking processes. The bending and blanking processes were done on the same workpiece to determine any changes in mechanical properties from one process to the other. As for bending, two pieces were cut so that the deformation could be investigated both along and across the drawing direction.

The same dies used in the verification experiments for deep drawing processes were also used in the verification experiments for deep drawing process were also used here for deep drawing as well. As for the bending and blanking processes the dies were modified to suit the size and shape of process component.

##### **4.4.1 Experimental Results of the Full Forming Process**

The data that was generated from the Angela system was processed to obtain force displacement graphs which were plotted using Microsoft Excel. The focus in this set of experiments was the forces causing deformation. The ram movement with respect to time was not considered as an important factor at this stage. The interest was to compare the deforming force before and after undergoing other processes.

##### **4.4.2 Deep Drawing**

The deep drawing process produced graphs that are shown in Figures 4.9 and 4.10 and highlighted no noticeable variations since it was the first process to be performed on the material. Before drawing a material, the workpiece is first blanked from the parent sheet to produce a piece to suit the desired shape. The

absence of variations in the material properties and/or deformation behaviour in this first process was an indication that blanking to produce the workpiece for this process did not have any effect on the workpiece.

#### 4.4.3 Bending

The bending forming process was applied on a work piece that was cut off the deep drawn part described in the previous section. This option was adopted to avoid the complicated flanging design requirements of a die for a cup-shaped piece. Two work pieces were cut, workpiece 1 and workpiece 2 from parent sheet and deep drawn product respectively.

Figure 4.14 gives a comparison of the variation of the punch forces with deformation for a workpiece that did not undergo deep drawing deformation before being exposed to bending and the other workpiece which was exposed to bending after undergoing a deep drawing process.

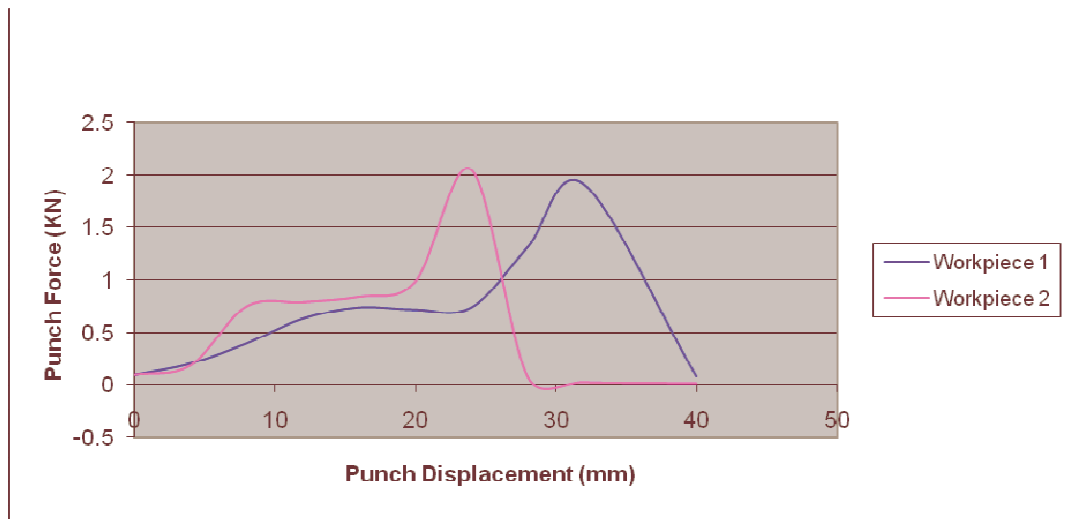


Figure 4.14: Comparison of Punch Forces

Workpiece 1 represents the material that went through the bending process without any prior deep drawing on it. The other one, workpiece 2 under went deep drawing process before being subjected to bending.

The graphs shown in Figure 4.14 were generated by superimposing data from workpiece 1 and workpiece 2. From the graphs it can be seen that the maximum force (2.1 kN) reached for the material that had undergone deep drawing prior to bending is slightly higher than that for the material that was bent without previously being deep drawn which recorded a maximum force of 2 kN. This represents a 5 percent increase in punch force.

#### 4.4.4 Blanking

Similarly, the blanking process was carried out on a piece cut from the deep drawn cup and then subjected to bending. Figure 4.15 shows the punch force against punch displacement during blanking for materials with and without prior deep drawing.



Figure 4.15: Comparison of Blanking Forces

The blanking force obtained from workpiece 2 was approximately 325kN compared to 300kN for workpiece 1. This represents an 8% increase in the blanking force due to work hardening.

#### 4.4.5 Coupling Simulations

Figure 4.16 shows a Forming Limit Diagram (FLD) plot of the major and minor strains in a blanking process. The strains are predominantly of stretch forming characteristic up to material failure. Both the major and minor strains can be seen to be predominantly unidirectional and continue to increase in magnitude until the material ruptures. Comparing with Figure 3.5, the higher strains obtained were in a region (D) of severe thinning an indication of failure.

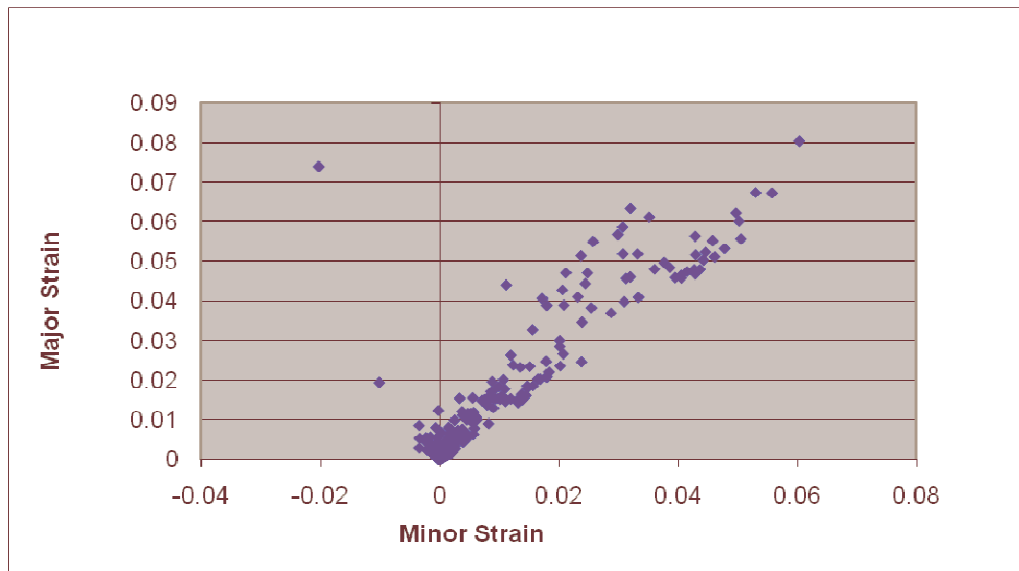


Figure 4.16: FLD of Major Strain against Minor Strain in a Blanking Process

In deep drawing simulation results shown in Figure 4.17, a combination of strains obtained lied above the lines  $\epsilon_1 = \epsilon_2$  and  $\epsilon_1 = -\epsilon_2$  indicating that a material had undergone stretch forming and deep drawing respectively. The higher concentration of strains obtained were around the origin in the recommended region (A) for forming processes.

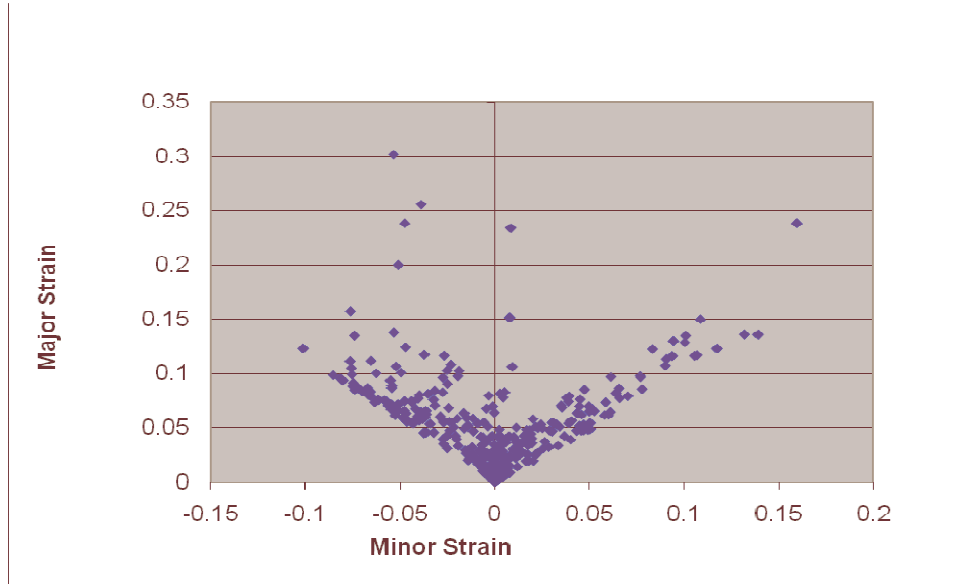


Figure 4.17: FLD of Major Strain against Minor Strain in a Deep Drawing Process

Figure 4.20 shows that the bending strains obtained were more confined along the line  $\epsilon_1 = \epsilon_2$  and closer to region E (Ref. Figure 3.5) a region of insufficient plastic strain and risk of spring back. The uniaxial tensile strains were also present with a few falling in a region of plane strain. This indicates that the material underwent tensile and compressive strains on the outer and inner regions of the workpiece respectively.

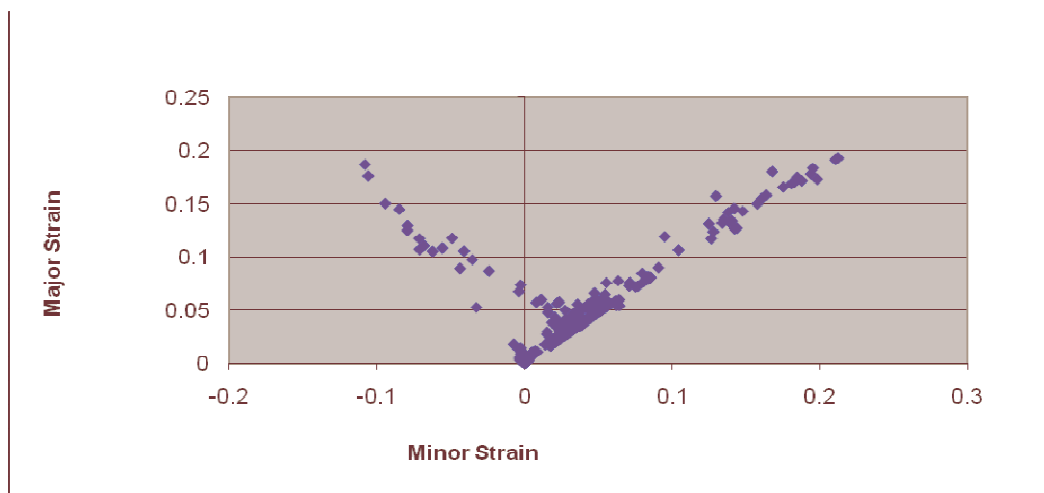


Figure 4.18: FLD of Major Strain against Minor Strain in a Bending Process

In the manufacture of sheet metal components, various forming and cutting processes are used. The production line will typically comprise a sequence of blanking, deep drawing and bending processes. Usually the first process to be carried out will be blanking followed by deep drawing. Superimposing the strain state of the two processes will usually help assess the formability of sheet metals through these processes.

Figure 4.21 shows the combined FLD for the deep drawing and blanking processes. The plane strains ( $\epsilon_1 = 0$ ) obtained are not high enough to fall in the regions that can cause failure regions B and C). Most of the blanking strains act in a different direction,  $\epsilon_1 = 0$ , and hence do not have significant or no affect on the subsequent process.

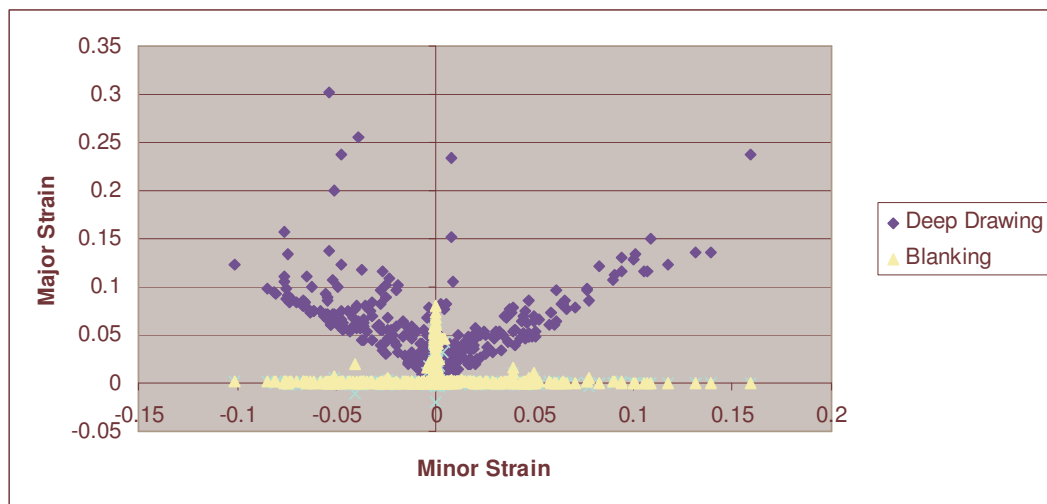


Figure 4.19: Combined FLD of a Blanking & Deep Drawing Process

After a deep drawing process the products would normally undergo some form of bending for example during flanging or hemming. The strain combination of these processes is shown in Figure 4.20 It can be observed in the figure that the major strain dominates in the bending process compared to deep drawing.

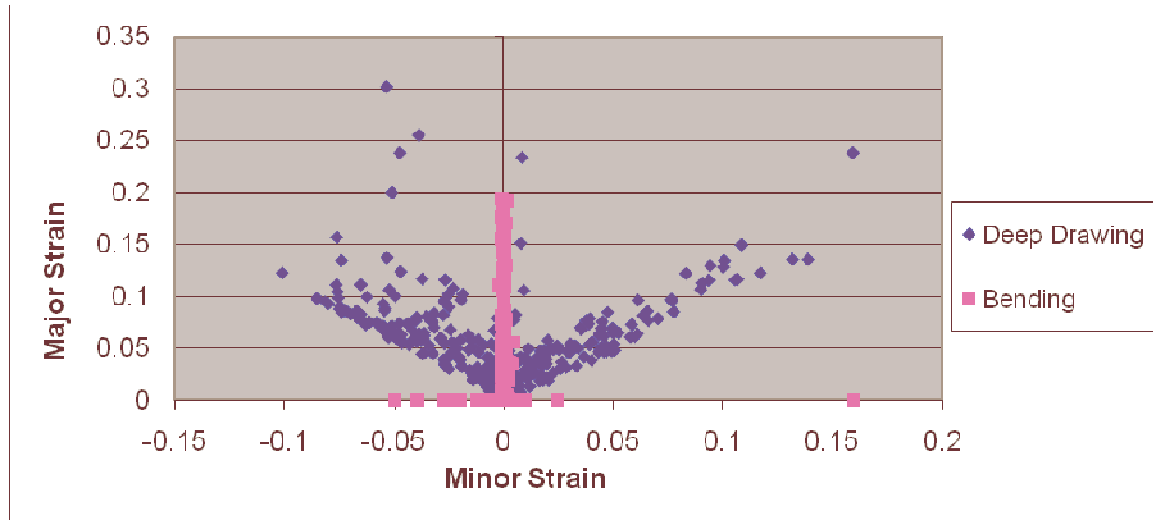


Figure 4.20: FLD of the Deep Drawing and Bending Processes

As stated above, if a workpiece undergoes a deep drawing process followed by bending, plane strain,  $\epsilon_2 = 0$  dominates in a material. The magnitude of the resulting plane strain could cause cracking once they fall in regions B and C. Therefore, after deep drawing the material is likely to develop some cracks around the bend area during the subsequent processes of flanging or hemming.

Combining the three processes, shown in Figure 4.21, indicate that a material undergoing multiple forming processes requires thorough investigation of formability in areas of the blank affected by the processes. If for example flange slitting is required on a deep drawn component, then a much high force is required due to the work hardened edge resulting from the blanking process.

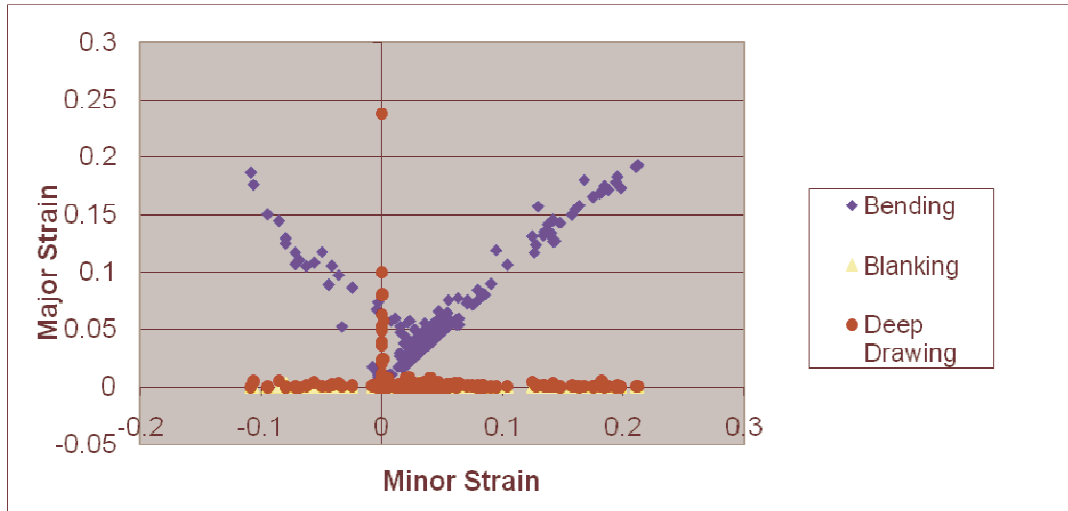


Figure 4.21: FLD of Combined Blanking, Deep Drawing and Bending Processes

From the FLD diagrams presented above, it is clear that the deep drawing process undergoes a much more complex strain combination with strains that are generally of much higher magnitude than the other processes. This process should therefore be the basis for failure design of the combined blanking, deep drawing and bending processes.

## CHAPTER 5

### DISCUSSION

#### 5.1 Introduction

Simulated and experimental punch forces for the blanking, deep drawing and bending processes are compared. There is a generally good agreement between simulated and experimental forces. During experimentation more attention was paid to lubrication so as to have conditions closer to those of the simulation. In all simulations, the friction coefficient was seen to be very sensitive and can give wrong results if not properly selected.

The differences that were observed between the simulated results and the experimental ones can be attributed to various factors that include the difficulty in accurately modelling the forming processes studied here. It was not possible to replicate all the physical conditions of the forming processes in the simulation model. Also accurate material modelling that would exactly depict the material behaviour as it undergoes deformation is difficult to achieve. On the other hand, the sheet metal may have had its properties changed due to storage, handling and rolling during sheet metal production. For example if the material was stored in a place where temperature range was relatively high, then the properties definitely may have been altered. As for the rolling during sheet metal production, the resulting preferred grain orientation has a significant effect on the forming loads depending on whether deformation bending is along or across the grain orientation. This however was not captured in computer simulation during material modelling.

The other constraint faced when modelling was related to work hardening of the material during processing and sliding conditions between the workpiece and the die although a workpiece hardening factor of 0.85 (Table 3.1) was used in the simulations. This could not account for the actual work hardening since it is an average value. In order to minimise the effects of all these shortcomings in

modelling, several runs are normally done with adjustments of the model parameters after each run before settling on a final model.

The accuracy of the simulations could have been affected by the mesh size. Proper workpiece mesh can make model produce more reliable results. Simulating the same model with smaller shell elements may make the model more accurate. However, trying different meshes takes a long time. This is one of the big problems of simulations in that time is limited. Simulating with computer with a larger memory or even parallel connected computers could be a good solution to decreasing simulation time. A possibility to save simulation time is to mesh the model with smaller elements in the area of study. Blank area around punch and die could be meshed differently than the boundaries.

The elasto-plasticity model produced reliable results to a certain degree of accuracy. This may be improved by choosing the correct element size. A mesh with smaller elements gives more accurate results but at the expense of simulation time and computer memory. Adjusting the mesh size was a good option to make the model more accurate and save simulation time. However, this was limited by the computer capacity that was used. As noticed, the results have been greatly influenced by the mesh.

The material model also has a significant effect on the simulation results. The material model used in all simulations in this study was a solid element model.

In order to ensure the model reliability, experimental tests were carried out so as to enable readjusting the model hence improving it. This kind of feedback is important to make the model represent the true behaviour of the material as it undergoes any sheet metal forming process.

## **5.2 The Blanking Process**

In calculating the cutting forces, it was assumed that the bottom of the punch and the top of the die block lie in the parallel planes. This meant that the sheet metal was sheared simultaneously along the whole perimeter. As a result the

shearing process was characterised by very high punch forces exerted over a very short time, resulting in a shock or impulse loading condition. However, this expected shock or impulse loading was not evident in the data more so the simulation results for blanking. Figure 4.2 showed a fairly sharp peak for experimental work, but no well defined peak for the predicted simulation results. The lack of conformity of the experimental results obtained to the expected results is likely to have been due to the ductility of the workpiece material used.

From Equation 4, the theoretical blanking force,  $F$ , can be calculated as follows for a punch diameter  $D = 121\text{mm}$ , a blank thickness  $t = 1.6\text{mm}$ , shear strength of the sheet material  $\tau_s = 350\text{MPa}$ . and a factor  $k$  of unity:

$$F_{\max} = \pi * 121 * 1.6 * 350$$

Giving  $F_{\max} = 212.9 \text{ KN}$

This theoretical force of 212.9 kN is lower than the value of 275 kN shown in Figure 4.8 that was obtained from both the simulation and experimental work done here. The calculated force (theoretical) was used as a starting point (force) in the force simulation.

As has been stated in section 3.3, the factor  $k$  takes care of the work hardening of the material during deformation, material non-homogeneity of the sheet metal, amount of clearance between the punch and die and the state of the cutting edge and is determined experimentally. Substituting a real value of the factor  $k$ , instead of arbitrarily equating it to unity, brings the theoretical value closer to the experimental and simulated values.

The experimental and simulated values both gave a peak force of 275 kN, though at different punch penetrations. As can be seen from Figure 4.8, in the experimental graph, punch penetration was delayed for about 0.5mm compared to the case for simulation probably due to work hardening of the blank as

deformation occurred. The effect of work hardening is not taken care of in simulations.

### 5.3 The Deep Drawing Process

The contour plot of the von Mises stresses (Figure 4.5) shows that the portion subjected to forming experienced a stress of magnitude ranging from 241 MPa to 482 MPa. Since the initial yield stress of the material is 282.7 MPa., the above values of stress indicate that the material underwent plastic deformation. The higher stress levels obtained here are significantly much higher than the yield stress and are likely to fall well beyond the range of uniform plastic elongation. As expected, these stresses fall way beyond the ultimate tensile stress of 420 MPa. for the sheet material used. The stresses in a material undergoing deep drawing should be confined to the region of plastic elongation and regions of necking and non-uniform deformation should be avoided.

The theoretical deep drawing force can be calculated from Equation 5 by substituting the values of cross sectional area  $A_s = \pi \cdot 100 \cdot 1.6 = 502.72 \text{ mm}^2$ , yield strength in tension  $\sigma_y = 282.685 \text{ Mpa}$ , ratio of blank to sheet diameters,  $D/d = 100/59.4 = 1.6835$  and assuming a value for the friction and bending constant,  $C = 0.6$  (Sharma, 2003). thus

$$F = 502.72 * 282.685 \left( \frac{100}{59.4} - 0.6 \right) = 153.98 \text{ kN}$$

The maximum force recorded in the experimental and simulation deep drawing processes shown in Figure 4.10 to be 285 kN and 275 kN respectively. Both these maximum forces and the forces during the entire process compare well as is evident from the figure. The maximum forces are however very different in magnitude from the theoretical deep drawing force calculated from the equation above. This difference can be attributed to the average value of the constant  $C$ , used in the equation which is dependant on die angle and the friction/lubrication.

## 5.4 The Bending Process

Bending, like most forming processes, involves using stress below and above the yield strength of the material. The strains in bending are therefore both plastic and elastic. The plastic strain accounts for the larger part of deformation in bending. The elastic strain is recovered after retraction of the bending tool in the form of spring back.

Comparing the bending force from simulation with the experimental work highlights similarity of the punch pressure versus displacement curve profiles, with differences in both the magnitude of the curves and the location of the peaks. The results can be considered to be reliable within experimental errors. The experimental maximum force occurred at a punch penetration of 20 mm while for the simulation peak force at 12 mm as shown in Figure 4.13. The delay in reaching the peak force during experimentation could be attributed to the work hardening of the material during processing.

The theoretical bending force can be calculated from Equation 6, by substituting the bend length  $l$  of 50 mm, the ultimate tensile stress of 420 MPa, the width of the die opening  $w$  of 50 mm and the blank thickness  $t$  of 1.6 mm to give

$$F = 1.2 \cdot \frac{50 * 1.6^2 * 420}{50} = 1.29 \text{ kN}$$

The experimental and simulated forces were 1.9 kN and 1.5 kN, respectively. The theoretical value of 1.29 kN is in close agreement with the simulated value but lower than the experimental force by 32% due to the assumed factor of 1.2 which accounts for friction and the die profile.

## 5.5 Coupling Simulations

The combined FLD of the blanking, deep drawing and blanking processes shown in Figure 4.21 indicate that when the three processes are coupled, the areas affected by both bending and deep drawing require a critical analysis.

The bending process which is predominately plain strain,  $\epsilon_2=0$ , and deep drawing which combines stretch forming  $\epsilon_1=\epsilon_2$  and  $\epsilon_1=-\epsilon_2$  (see Figure 3.5) clearly indicate that the strains involved in both processes are high and if not controlled can cause failure if applied on the same work piece area. Therefore, the strains generated from the bending process need to be limited within the recommended region, A, shown in Figure 3.5. This is very possible when drawing complicated shapes. The clustering of the strain around the origin is a good sign that the workpiece is safe, and this is a recommended region for forming processes (region A from Figure 3.5).

As can be seen from Figure 4.21, blanking can only become an issue of concern when other processes are to be performed along or close to the blanked edge since all the strains fall in areas where there is insufficient plastic strain, the regions marked E and G in Figure 3.5.

From the combined FLD shown in Figures 4.19, 4.20 and 4.21, limiting strains in a material can be used to assess formability of the workpiece as it moves from one forming stage to the other.

The coupling of simulations therefore greatly helps to assess the strains in a material as it moves from one forming stage to the other to ascertain its formability. The assessment can help a die designer to adjust parameters based on the strain state of the material for the subsequent process under design.

## CHAPTER 6

### CONCLUSIONS AND RECOMMENDATIONS

#### 6.1 Conclusions

- The blanking, deep drawing and bending models developed for the simulation were in good agreement with the experimental results.
- The contours of stress and strain distribution obtained in all three simulations gave a precise location on a workpiece as expected theoretically. The results were in good agreement with the experiments.
- Blanking has less or no impact on subsequent processes.
- A combination of deep drawing and bending processes has been identified as major strain contributors in a production line.
- In a full deep drawing process, deep drawing should be used as a basis for subsequent process.

#### 6.2 Recommendations

- The other method of coupling simulations using finite element package with multi-physics platform will be worth trying. The multi-physics platform basically compares the strains in the forming limit diagram digitally.
- The results can be improved by developing an algorithm for coupling simulations.

## REFERENCES

Arwidson, C., "Numerical Simulation of Sheet Metal Forming", Lulea University of Technology, PhD Thesis 2005.

Budianky, B., and Wang, N.M., "On the Swift Cup Test," Journal Mechanical Physical Solids, Vol. 14, 1966, pp. 357-374.

Bunssen C. and Wohlmuth J., "Incremental Simulations and Modeling of Bending of Sheet, J. Mater. Processing Tech. 39 2006, pp. 279-300

Chiang, D.C., and Kobayashi, S., "The Effect of Anisotropy and Work Hardening Characteristic On the Stress and Strain Distribution in Deep Drawing", ASME Journal for Engineering for Industry. Vol. 88 No. 4, Nov. 1966, pp 443-448

Chuan W, Gary K. and Taylan A., "Mathematical modeling of plane-strain bending of sheets and plates," Journal of . Material .Processing Technology., vol. 39, pp 279-304, 1993.

Chung, S. Y., and Swift, H. W., "Cup Drawing from a Flat Blank," Proc. Of the Institute of Mechanical Engineers," Vol. 165, 1951, pp. 193-223.

Danckert J. (2004) Experimental and FEM analysis of a Combined Deep Drawing and Ironing Process. Ph.D. Thesis, Department of Production, Aalborg university pp133-140.

Date P., Narasimhan K, Maiti K and Singh P, "On the prediction of spring back in Vee- Bending of metallic sheets under plane strain condition," Sheet Metal, Sept 1999, pp 447-456.

David J. G., "Prediction of Localised Fracture in a Bending process" Journal of material Process Technology. Vol 58, pp. 20-23, 1996

Dieter G., "Mechanical Metallurgy", McGraw Hill, Metric Edition, London, 1988. pp 212-215

Gaier C., Kose K., Hebisch H. and Pramhas G., 'Coupling Forming Simulations and Fatigue Life Predictions of Vehicle Components', MAGNA STEYR, Engineering Center Steyr, Valentin, Austria, 2004. pp. 65-68.

Gandhi A. H., G. J. Solanki and H. K. Raval, "Investigation on Multiple Pass Bending-A Simulation Study," Proc. Int. Conf.on Recent Advances in Mechanical & Materials Engg., Kuala Lumpur, Malaysia, 30-31 May 2005, pp. 971-976.

Gandhi A. H., G. J. Solanki and H. K. Raval, "On the effect of various parameters on springback and energy in multiple pass (Air vee) bending: part 1," Proc. 3rd Int. conf. on manufacture. Research (ICMR2005), Cranfield University, UK, 6-8 Sept 2005

Gantner. S, and Bauer. N, "Experimental and Numerical Prediction of Springback and Side Wall Curl in U-Bending of Isotropic Sheet Metals", Journal of Material Processing Technology 105, 1999 pp. 382-393.

Gedney R., "Tensile Testing for Determining the Formability of Sheet Metals", ADMET Report, Inc, Norwood, Massachusetts, 2002, pp. 24-31

Ghouati O., and Chen X., "Sheet Metal Forming Simulations-Closing the Design Loop". Ford Research and Advanced Engineering Europe Conference, Germany. 2006. pp.16-21

Gokhale, F, " Recent Progress on the Understanding of Hydroforming Process", Metal Forming Process, ed. The Metallurgical Society, USA, 2002, pp. 134-146

Goodwin G. and S. Tsang, "The Plastic Bending of beams Considering Die Friction Effects," Transaction of ASME, J. Eng. Ind., pp. 237-250, August 1986.

Grieve D., "Manufacturing Processes – 3 Metal Forming," Journal of Engineering for Industry, March 17, 1996, pp 23-36

Hedrick, A, "Designing high-strength steel stamped parts for formability". Journal of Material Technology, Vol. 85, pp. 84-100, 2003.

Hill, R., "The Mathematical Theory of Plasticity, Oxford, Clarendon Press, 1950. Pp 27-35

Hosford W. 'Metal Forming, Mechanics and Metallurgy, University of Michigan, 1983. Mc

Inamdar M. V., P. P. Date, K. Narsimhan, S. K. Maiti and U. P. Singh, "Development of Artificial Neural Network to predict springback in air V bending," Journal of Advanced Manufacturing Technology., vol. 16, pp. 376-381, 2000.

Jain N., Shi X., Ngaile G., Altan T., Pax B., Harman B. and Homan G., "Simulation Confirms Deep Drawn Die Design", Metal Forming Magazine, November 2003 Issue. pp. 51-56

Jenn-Terng Gau and Gary L. Kinzel, "An Experimental Investigation of the Influence of the Bauschinger Effect on Springback Predictions," Journal of Material Process Technology, vol. 108, pp. 369-375, 2001.

Kalpakjian P. and Schmid V. "CustomPartNet" , Wikipedia, 2008.

Keeler, V. "Modeling of Strain Distribution in Biaxial Stretching of Sheet Metal Forming Process", The Metallurgical Society, USA, 1988, pp.129-134.

Keeler, V. and Backofen. G. "Computer Modeling of Sheet Metal Forming Process", The Metallurgical Society, USA, 1985, pp.259-271.

Kobayashi S., Oh S.I. and Altan T., 'Metal forming and the finite method', Oxford University Press, New York, 1989. pp. 23-35

Leu, D. " A simplified Approach for Evaluation of Bendability of Anisotropic Sheet Metals, "Journal of Materials Processing Technology," 66, pp 9-17,1997

Menders T., "Simulation of Sheet Metal Forming Process". <http://tmku209.ctw.utwente.nl/~timo/> [LS-DYNA Keyword Users Manual, Version 970, Livermore Software Technology Corporation (LSTC), April 2003. International Journal of Mechanical Systems Science and Engineering Volume 1, Number 2122

Odell, E. I., PhD. Thesis, Department of Engineering Mechanics, The Ohio State University, 1973.

Panknin, D, "Design Optimisation of Deep Drawing Process", ASME Journal of Engineering for Industry Vol. 112, February 2002.

Park Y. and Colton J.S., "Failure Analysis of Rapid Prototyped Tooling in Sheet Metal Forming-V-Die Bending", ASME Journal of Achievements in Material Manufacturing Engineering Vol. 127, February 2005.

Picart D. "Investigation of the Damage Mechanism in a Blanking Process", Journal of Material Process Technology. Vol. 56, pp18-25 1995

Rahaul, V., and Haldar, K., "A Sensitivity Analysis for the Optimal Design of Metal-forming Processes" Comput. Methods Appl. Mech. Eng. Vol. 129, pp 339-348, 2003.

Rowe G., "Principles of Industrial Metal Working Processes", Edward Arnold, 1977., pp 46-70.

Sachs, G., "New Research on the Drawing of Cylindrical Shells," "Pro. Of the Institute of Automobile Engineers, Vol. 29, 1934, pp.588-600

Schuler. E, "Metal Forming Handbook. 1998. Engineering Research Centre for Net Shape Manufacturing". The Ohio State University, USA. Ed.

Seo Y, "Simulation Beats Trial-and-Error", Metal Forming magazine, May 2002 Issue, pp. 66-69

Sharma C, "A Textbook of Production Engineering,' Chand & Company, New Delhi, 2003, pp. 165-168

Siebel, E., and Pomp, A., "The Mechanics of Sheet Metal Forming," Edward Arnold Ltd., London, 1932, pp. 270-276

Stoughton, B. "Experimental and Numerical Investigation of Bending Process", Journal of Material Processing Technology. Vol. 57 pp 90-77, 1960.

Vin de J, A, Streppel H, Singh P and Kals J, "A process model for air bending," Journal of Material Process Technology., vol. 57, pp. 48-54,1996.

Woo, M., "On the Complete Solution of a Deep Drawing Problem," International Journal of Mechanical Science, Vol. 10, 1996, pp. 83-94.

Xuechun. L, Yuying. Y, Yongzhi. W, Jun. B and Shunping L, "Effect of Material Hardening Mode on the Springback Simulation Accuracy of V-free Bending," Journal of Material Processing Technology, vol. 123, pp. 209-211, 2002.

## APPENDIX 1. Simulated Results

### Blanking

Z (mm)	Punch Force (KN)				
31.417	1.77E-01	27.123	8.87E+01	20.083	1.70E+02
31.417	2.68E-01	27.055	1.76E+02	19.995	1.46E+02
31.417	8.34E-01	26.144	1.77E+02	19.698	1.49E+02
31.417	3.13E-01	25.264	2.89E+01	19.606	1.27E+02
31.417	1.87E+00	25.232	1.29E+02	19.566	1.68E+02
31.417	1.60E+02	25.232	1.40E+02	19.555	7.36E+01
31.417	1.55E+02	25.232	1.56E+02	19.509	2.56E+02
31.417	1.56E+02	25.232	1.62E+02	19.377	1.55E+02
31.417	1.60E+02	25.232	1.69E+02	19.15	1.65E+02
31.417	1.65E+02	25.232	1.74E+02	19.112	2.29E+01
31.417	1.69E+02	25.232	1.75E+02	19.048	1.70E+02
31.417	1.73E+02	25.232	1.74E+02	18.987	1.89E+01
31.417	1.75E+02	25.232	1.71E+02	18.865	1.66E+01
31.417	1.77E+02	25.232	1.66E+02	18.796	1.60E+02
31.417	1.78E+02	25.232	1.59E+02	18.689	1.73E+02
31.417	1.74E+02	25.232	1.51E+02	18.33	1.74E+02
31.417	1.71E+02	25.232	1.31E+02	18.216	1.60E+02
31.417	1.67E+02	25.193	2.07E+01	18.044	1.34E+02
31.417	1.62E+02	25.122	1.76E+01	17.996	3.34E+02
31.417	1.57E+02	25.035	2.86E+02	17.895	1.28E+02
31.417	1.53E+02	24.874	1.77E+02	17.696	3.99E+01
31.417	1.56E+02	24.073	1.31E+02	17.395	1.50E+02
31.417	1.58E+02	24.047	4.82E+01	16.892	1.45E+02
31.417	3.09E+02	23.974	2.89E+02	16.777	1.52E+02
31.417	1.95E+02	23.962	1.77E+02	16.567	1.42E+02
31.417	4.34E+01	23.932	1.68E+02	16.508	1.68E+02
31.417	2.01E+01	22.923	1.46E+02	16.482	1.27E+02
29.236	1.77E+02	22.923	1.46E+02	16.473	1.69E+02
29.236	1.77E+02	22.914	1.64E+02	16.32	2.30E+02
28.341	4.54E+01	22.829	8.63E+01	16.28	5.48E+01
28.341	2.89E+01	22.692	1.77E+02	16.149	1.56E+02
28.325	1.77E+02	22.658	1.69E+02	16.149	1.73E+02
28.325	1.74E+02	22.658	1.72E+02	16.036	2.17E+01
28.325	1.74E+02	22.419	1.29E+02	15.956	1.65E+02
28.325	1.71E+02	22.419	1.25E+02	15.897	1.90E+01
28.325	1.69E+02	22.305	1.58E+02	15.763	1.65E+01

28.325	<b>1.67E+02</b>	22.305	<b>1.57E+02</b>	15.569	<b>1.58E+02</b>
28.325	<b>1.65E+02</b>	22.272	<b>2.43E+02</b>	15.54	<b>1.58E+02</b>
28.325	<b>1.61E+02</b>	22.188	<b>2.58E+01</b>	15.005	<b>1.74E+02</b>
28.325	<b>1.59E+02</b>	22.14	<b>1.75E+02</b>	14.973	<b>1.57E+02</b>
28.325	<b>1.56E+02</b>	22.14	<b>1.74E+02</b>	14.806	<b>2.99E+02</b>
28.325	<b>1.54E+02</b>	22.064	<b>2.03E+01</b>	14.705	<b>1.14E+02</b>
28.325	<b>1.52E+02</b>	21.987	<b>1.71E+01</b>	14.62	<b>3.74E+01</b>
28.325	<b>1.49E+02</b>	21.781	<b>1.76E+02</b>	14.178	<b>1.55E+02</b>
28.325	<b>1.44E+02</b>	21.724	<b>1.61E+02</b>	13.968	<b>1.65E+02</b>
28.325	<b>1.31E+02</b>	21.724	<b>1.63E+02</b>	13.853	<b>1.59E+02</b>
28.269	<b>2.03E+01</b>	21.26	<b>1.14E+02</b>	13.55	<b>1.51E+02</b>
28.267	<b>1.77E+01</b>	21.211	<b>2.37E+02</b>	13.528	<b>1.72E+02</b>
<b>28.226</b>	<b>2.37E+02</b>	21.169	<b>1.31E+02</b>	13.416	<b>1.65E+02</b>
28.226	<b>3.06E+02</b>	20.971	<b>4.39E+01</b>	13.324	<b>1.78E+02</b>
28.226	<b>1.63E+02</b>	20.613	<b>1.44E+02</b>	13.131	<b>2.37E+02</b>
27.165	<b>1.76E+02</b>	20.511	<b>1.78E+02</b>	13.045	<b>4.54E+01</b>
12.959	<b>2.05E+01</b>	20.109	<b>1.35E+02</b>		
12.922	<b>1.52E+02</b>	6.9527	<b>3.42E+02</b>		
12.863	<b>1.58E+02</b>	6.9425	<b>1.53E+02</b>		
12.821	<b>1.83E+01</b>	6.8066	<b>1.77E+01</b>		
12.685	<b>1.65E+01</b>	6.7129	<b>1.69E+01</b>		
12.326	<b>1.52E+02</b>	6.6787	<b>1.41E+02</b>		
12.297	<b>1.56E+02</b>	6.621	<b>1.59E+01</b>		
11.848	<b>1.81E+02</b>	6.5611	<b>9.40E+01</b>		
11.787	<b>1.63E+02</b>	6.5152	<b>4.45E+01</b>		
11.73	<b>1.51E+02</b>	6.2545	<b>1.56E+02</b>		
11.649	<b>3.32E+02</b>	5.9611	<b>1.46E+02</b>		
11.471	<b>1.11E+02</b>	5.8877	<b>1.37E+02</b>		
11.385	<b>3.29E+01</b>	5.2435	<b>1.51E+02</b>		
11.234	<b>1.60E+02</b>	5.1499	<b>1.93E+02</b>		
11.107	<b>1.56E+02</b>	5.0131	<b>2.19E+01</b>		
10.783	<b>1.77E+02</b>	4.8904	<b>7.45E+01</b>		
10.276	<b>1.50E+02</b>	4.7813	<b>1.88E+02</b>		
10.216	<b>1.58E+02</b>	4.0623	<b>1.21E+02</b>		
10.167	<b>2.39E+02</b>	3.8903	<b>1.71E+02</b>		
9.8829	<b>1.88E+01</b>	3.7799	<b>1.35E+02</b>		
9.8461	<b>1.56E+02</b>	3.7585	<b>1.63E+01</b>		
9.8108	<b>4.76E+01</b>	3.7387	<b>2.90E+02</b>		
9.7892	<b>1.80E+01</b>	3.6441	<b>1.58E+01</b>		
9.771	<b>1.52E+02</b>	3.5864	<b>1.33E+02</b>		

9.6804	<b>1.48E+02</b>	3.3743	<b>1.38E+02</b>
9.6363	<b>1.61E+01</b>	3.2196	<b>3.52E+01</b>
9.6057	<b>1.62E+02</b>	3.2006	<b>6.40E+01</b>
9.588	<b>1.53E+02</b>	3.0623	<b>1.44E+02</b>
9.2045	<b>1.51E+02</b>	2.8993	<b>1.30E-03</b>
9.1016	<b>8.89E+01</b>	2.6324	<b>3.03E-03</b>
9.0534	<b>1.53E+02</b>	1.9649	<b>2.07E-03</b>
8.3639	<b>2.40E+02</b>	1.7894	<b>9.86E-03</b>
8.3087	<b>2.93E+01</b>	1.5298	<b>5.44E-03</b>
8.186	<b>8.07E+01</b>	1.526	<b>1.71E-03</b>
8.0367	<b>2.00E+02</b>	0.88122	<b>1.29E-03</b>
7.6304	<b>1.41E+02</b>	0.71028	<b>1.60E-03</b>
7.4246	<b>1.59E+02</b>	0.68765	<b>1.25E-03</b>
7.1545	<b>1.45E+02</b>	0.53509	<b>1.31E-03</b>
7.1456	<b>1.59E+02</b>	0.49409	<b>1.14E-03</b>
		0.44342	<b>2.10E-03</b>
		0.019113	<b>1.08E-03</b>

### Deep Drawing

Step	Von Mises (Pa)		
		50	797.2
1	466.9	55	808.2
5	605.8	60	811.7
10	638.1	65	812.2
15	692.9	70	809.5
20	711.9	75	815.2
25	724.4	80	809.6
30	739.7	85	800.5
35	758.5	90	782.3
40	774.3	95	779.8
45	788.6	100	780.4
		104	780.3

## Bending

Displacement (mm)	von Mises (N/m <sup>2</sup> )	Punch Force (KN)
0	7.16E+07	1.22E-01
2.5	1.18E+08	2.00E-01
5	2.07E+08	3.52E-01
7.5	2.82E+08	4.79E-01
10	5.99E+08	1.02E+00
12.5	9.21E+08	1.56E+00
15	5.72E+08	9.72E-01
17.5	4.87E+08	8.28E-01
20	3.49E+08	5.93E-01
22.5	3.06E+08	5.20E-01
25	3.19E+08	5.42E-01
27.5	3.18E+08	5.41E-01
30	2.75E+08	4.67E-01
32.5	2.25E+08	3.83E-01
35	2.46E+08	4.17E-01
37.5	2.47E+08	4.19E-01
40	2.75E+08	4.67E-01

## APPENDIX 2 Experimental Results

### Blanking

Time ms	Displacement (mm)	Pres. (N/mm <sup>2</sup> )	Time (ms)	Displacement (mm)	Press. (N/mm <sup>2</sup> )
0	76.575	0.38985	5400	13.33	1.168034
100	76.575	0.117659	5500	12.048	1.162987
200	76.575	0.118169	5600	10.73	1.160967
300	76.575	0.118169	5700	9.448	1.159953
400	76.575	0.120189	5800	8.13	1.15945
500	76.538	0.650926	5900	6.848	1.159953
600	75.659	1.314986	6000	5.53	1.160967
700	74.304	1.108447	6100	4.614	1.89572
800	73.022	1.155408	6200	2.563	0.469133
900	71.704	1.145817	6300	1.648	1.318519
1000	70.422	1.152884	6400	0.623	1.046334
1100	69.104	1.158441	6500	0.623	1.152383
1200	67.822	1.161468	6600	0.623	0.545892
1300	66.541	1.163488	6700	0.623	0.529731
1400	65.222	1.165005	6800	0.623	0.539328
1500	63.904	1.164495	6900	0.623	0.542859
1600	62.585	1.163992	7000	0.623	0.545892
1700	61.304	1.164495	7100	0.623	0.546396
1800	60.022	1.164495	7200	0.623	0.547409
1900	58.74	1.163488	7300	0.623	0.400454
2000	57.422	1.165005	7400	2.856	0.135337
2100	56.14	1.162985	7500	5.383	0.209573
2200	54.858	1.161971	7600	8.24	0.170183
2300	53.54	1.161971	7700	10.95	0.178767
2400	52.258	1.161971	7800	13.77	0.174727
2500	50.977	1.161468	7900	16.296	0.17725
2600	49.622	1.161468	8000	19.08	0.17523
2700	48.267	1.161971	8100	21.863	0.175734
2800	46.985	1.160965	8200	24.573	0.178767
2900	45.667	1.160461	8300	27.393	0.178257
3000	44.385	1.161468	8400	30.103	0.180277
3100	43.066	1.161971	8500	32.849	0.179271
3200	41.785	1.161468	8600	35.559	0.181291
3300	40.54	1.161468	8700	38.379	0.176747
3400	39.221	1.162985	8800	41.089	0.178767
3500	37.903	1.162482	8900	43.762	0.180277
3600	36.511	1.162482	9000	46.509	0.178767

3700	35.229	1.163488	9100	49.219	0.17725
3800	33.948	1.163488	9200	51.965	0.17523
3900	32.666	1.165508	9300	54.053	0.176747
4000	31.348	1.164497	9400	56.799	0.174727
4100	30.066	1.16551	9500	59.509	0.169673
4200	28.784	1.163994	9600	62.219	0.171693
4300	27.502	1.162987	9700	64.966	0.170687
4400	26.184	1.162484	9800	67.712	0.166646
4500	24.866	1.16147	9900	70.459	0.168666
4600	23.584	1.16147	10000	73.242	0.16917
4700	22.266	1.16147	10100	75.952	0.185834
4800	20.984	1.160463	10200	76.831	0.075242
4900	19.702	1.161973	10300	76.831	0.073726
5000	18.384	1.160463	10400	76.831	0.076256
5100	17.102	1.162484	10500	76.831	0.076759
5200	15.784	1.16147	10600	76.794	0.077263
5300	14.502	1.160967	10700	76.831	0.077263
<b>Time (ms)</b>	<b>Displacement (mm)</b>	<b>Press. (N/mm<sup>2</sup>)</b>	10800	76.794	0.077263
10900	76.794	0.077263	<b>Time (ms)</b>	<b>Displacement (mm)</b>	<b>Pre (N/mm<sup>2</sup>)</b>
11000	76.831	0.076759	11700	76.831	0.075242
11100	76.794	0.076256	11800	76.831	0.074739
11200	76.794	0.076256	11900	76.831	0.074236
11300	76.794	0.076256	12000	76.831	0.074236
11400	76.831	0.075746	12100	76.831	0.073726
11500	76.831	0.075746	12200	76.831	0.073222
11600	76.831	0.075242	12300	76.831	0.072216
			12400	76.831	0.071705

## Deep Drawing

Time ms	Pressure (N/mm <sup>2</sup> )	Displacement (mm)	Time (ms)	Press. (N/mm <sup>2</sup> )	Displ. (mm)
0	1.276606	139.417	4100	1.160967	94.263
100	0.062618	139.417	4200	1.15945	92.981
200	0.063122	139.417	4300	1.159953	91.663
300	0.064135	139.453	4400	1.158443	90.344
400	0.079283	139.453	4500	1.160463	89.026
500	0.729707	139.417	4600	1.159953	87.708
600	1.209947	139.417	4700	1.162987	86.426
700	1.056939	138.831	4800	1.16349	85.107
800	1.115013	137.549	4900	1.163994	83.826
900	1.098852	136.23	5000	1.163994	82.507
1000	1.102389	134.912	5100	1.164497	81.152
1100	1.105416	133.667	5200	1.164497	79.871
1200	1.109959	132.349	5300	1.161973	78.589
1300	1.11198	130.957	5400	1.160463	77.271
1400	1.114	129.639	5500	1.158947	75.879
1500	1.11451	128.32	5600	1.15541	74.634
1600	1.118543	127.039	5700	1.152383	73.315
1700	1.11804	125.684	5800	1.149852	71.997
1800	1.119557	124.402	5900	1.146826	70.679
1900	1.120564	123.047	6000	1.143289	69.36
2000	1.121074	121.729	6100	1.138242	68.079
2100	1.12208	120.447	6200	1.133698	66.76
2200	1.125114	119.165	6300	1.133188	65.442
2300	1.127134	117.81	6400	1.132684	64.087
2400	1.130161	116.492	6500	1.132684	62.805
2500	1.131175	115.173	6600	1.132181	61.523
2600	1.132684	113.892	6700	1.132684	60.205
2700	1.136725	112.573	6800	1.132684	58.923
2800	1.137738	111.292	6900	1.132181	57.605
2900	1.142282	109.937	7000	1.131175	56.36
3000	1.145819	108.655	7100	1.131175	55.042
3100	1.149349	107.373	7200	1.129658	53.723
3200	1.152383	106.091	7300	1.131175	52.405
3300	1.153893	104.81	7400	1.130664	51.16
3400	1.154906	103.455	7500	1.129154	49.805
3500	1.15541	102.173	7600	1.155913	48.486
3600	1.155913	100.818	7700	1.252874	47.241
3700	1.156926	99.5	7800	1.311452	45.959

3800	1.158443	98.218	7900	1.379117	44.714
3900	1.160967	96.863	8000	1.449816	43.469
4000	1.160463	95.581	8100	1.480118	42.224
<b>Time (ms)</b>	<b>Press. (N/mm<sup>2</sup>)</b>	<b>Displ. (mm)</b>	<b>Time (ms)</b>	<b>Press. (N/mm<sup>2</sup>)</b>	<b>Displ. (mm)</b>
8300	1.5205146	39.661	10400	1.1003688	12.048
8400	1.5270784	38.379	10500	1.1084494	10.73
8500	1.5341524	36.987	10600	1.1124898	9.448
8600	1.5442532	35.669	10700	0.5928526	8.606
8700	1.5498035	34.424	10800	0.5630603	8.606
8800	1.5386961	33.105	10900	0.5766982	8.606
8900	1.5083936	31.787	11000	0.5827518	8.606
9000	1.4654737	30.469	11100	0.5888123	8.606
9100	1.3988152	29.15	11200	0.6484036	8.606
9200	1.3230694	27.832	11300	0.5378117	8.606
9300	1.2362093	26.477	11400	0.2428954	9.631
9400	1.1256174	25.122	11500	0.1883579	12.378
9500	1.093805	23.767	11600	0.2141167	15.198
9600	1.0857243	22.485	11700	0.1994722	17.981
9700	1.0796638	21.167	11800	0.193915	20.801
9800	1.0842075	19.849	11900	0.1822974	23.621
9900	1.081684	18.567	12000	0.1732101	26.404
10000	1.0867309	17.285	12100	0.1722035	29.187
10100	1.0897646	15.967	12200	0.1722035	31.97
10200	1.0907713	14.685	12300	0.1701833	34.753
10300	1.0948116	13.367	12400	0.1651294	37.573

## Experimental Bending Results

Time (ms)	Press. (N/mm <sup>2</sup> )	Displ. (mm)			
0	0.5463957	85.547	3000	1.130161	73.535
100	0.1353372	85.583	3100	1.133188	72.327
200	0.1312969	85.583	3200	1.136222	71.155
300	0.1242297	85.583	3300	1.137738	69.91
400	0.1161491	85.62	3400	1.132684	68.665
500	0.1116054	85.62	3500	1.122584	67.419
600	0.1242297	85.62	3600	1.117033	66.138
700	0.1479615	85.62	3700	1.115013	64.856
800	0.1636126	85.62	3800	1.117537	63.574
900	0.1913916	85.62	3900	1.117033	62.292
1000	0.2252241	85.62	4000	1.115013	61.047
1100	0.2731979	85.657	4100	1.116523	59.766
1200	0.3206683	85.657	4200	1.120564	58.521
1300	0.3676285	85.62	4300	1.128141	57.239
1400	0.4115618	85.657	4400	1.132684	55.957
1500	0.4696364	85.62	4500	1.136725	54.675
1600	0.5393286	85.62	4600	1.137738	53.394
1700	0.6276987	85.583	4700	1.144302	52.112
1800	0.7367738	85.547	4800	1.157933	50.83
1900	0.8771648	85.51	4900	1.165007	49.512
2000	1.0650194	85.437	5000	1.170054	48.157
2100	1.2947871	85.181	5100	1.166517	46.912
2200	1.2397463	83.789	5200	1.167531	45.593
2300	1.1271342	82.068	5300	1.168537	44.348
2400	1.0882478	80.676	5400	1.168537	43.066
2500	1.095717	79.468	5500	1.163994	41.785
2600	1.0968318	78.296	5600	0.00798	40.54
2700	1.1114762	77.161	5700	0.007928	39.258
2800	1.1210737	75.879	5800	0.007893	37.939
2900	1.1281409	74.78	5900	0.007879	36.621
6000	1.147832	35.339	9300	0.192398	45.776
6100	1.143799	34.131	9400	0.194418	48.523
6200	1.144805	32.849	9500	0.197955	51.343
6300	1.144302	31.567	9600	0.202499	54.053
6400	1.150363	30.286	9700	0.205533	56.763
6500	1.149852	29.004	9800	0.205533	59.473
			9900	0.206036	62.183

6600	1.148342	27.722	10000	0.221184	64.893
6700	1.147329	26.404	10100	0.227244	67.676
6800	1.149852	25.122	10200	0.231788	70.422
6900	1.154403	23.84	10300	0.227748	73.169
7000	1.159953	22.522	10400	0.228251	75.879
7100	1.162484	21.204	10500	0.228251	78.662
7200	1.161973	19.922	10600	0.227748	81.445
7300	1.162484	18.64	10700	0.224218	84.192
7400	1.176115	17.322	10800	0.21058	85.254
7500	1.190256	16.04	10900	0.200982	85.254
7600	1.03573	15.088	11000	0.196439	85.291
7700	0.997858	15.015	11100	0.196439	85.291
7800	0.999878	14.978	11200	0.192908	85.291
7900	1.002401	14.978	11300	0.180277	85.291
8000	1.003911	14.978	11400	0.176244	85.327
8100	1.000381	14.978	11500	0.172707	85.291
8200	0.718089	15.381	11600	0.178767	85.291
8300	0.401971	18.201	11700	0.178767	85.291
8400	0.304004	20.984	11800	0.179271	85.327
8500	0.2636	23.767	11900	0.180277	85.291
8600	0.242392	26.55	12000	0.184828	85.291
8700	0.217143	29.297	12100	0.191392	85.291
8800	0.206036	32.043	12200	0.197452	85.254
8900	0.196439	34.79	12300	0.200982	85.254
9000	0.199472	37.537	12400	0.203002	85.254
9100	0.196439	40.356			
9200	0.194418	43.066			

### Experimental Results for Deep Drawing -Full Process

Time (ms)	Press. N/mm <sup>2</sup>	Displ. (mm)			
0	0.113115	16.589	2200	1.160463	16.626
100	0.113619	16.626	2300	1.15743	16.626
200	0.110592	16.589	2400	1.154906	16.626
300	0.108068	16.626	2500	1.154403	16.626
400	0.105035	16.626	2600	1.152886	16.626
500	0.103015	16.626	2700	1.152383	16.626
600	0.101505	16.626	2800	1.151369	16.663
700	0.100491	16.626	2900	1.150363	16.626
800	0.099484	16.626	3000	1.149349	16.626

900	0.142404	16.626	3100	1.147832	16.626
1000	0.30299	16.626	3200	1.148342	16.663
1100	0.595383	16.626	3300	1.150866	16.663
1200	1.083704	16.626	3400	1.151873	16.626
1300	1.363969	16.626	3500	1.153389	16.626
1400	1.036737	16.626	3600	1.15541	16.626
1500	1.124101	16.626	3700	1.154906	16.626
1600	1.176115	16.626	3800	1.153893	16.626
1700	1.168537	16.626	3900	1.152886	16.626
1800	1.165007	16.626	4000	1.151369	16.626
1900	1.16551	16.626	4100	1.149852	16.626
2000	1.165007	16.626	4200	1.148342	16.626
2100	1.16349	16.626	4300	1.147832	16.626
4400	1.148846	16.626	10200	0.535288	5.017
4500	1.148846	16.626	10300	0.281782	4.724
4600	1.149349	16.626	10400	0.241385	4.504
4700	1.149349	16.626	10500	0.248453	4.431
4800	1.149852	16.626	10600	0.247446	4.395
4900	1.149349	16.626	10700	0.244412	4.431
5000	1.149852	16.626	10800	0.243909	4.395
5100	1.150363	16.626	10900	0.242392	4.431
5200	1.151873	16.626	11000	0.238862	4.431
5300	1.153893	16.626	11100	0.238862	4.395
5400	1.155913	16.626	11200	0.237345	4.395
5500	1.156926	16.626	11300	0.235828	4.431
5600	1.15743	16.626	11400	0.237848	4.431
5700	1.158947	16.333	11500	0.240372	4.395
5800	1.157933	15.637	11600	0.236842	4.431
5900	1.159953	14.832	11700	0.232801	4.431
6000	1.173591	14.136	11800	0.228251	4.358
6100	1.284183	13.513	11900	0.222701	4.175
6200	1.368513	13.074	12000	0.220177	3.992
6300	1.428104	12.708	12100	0.221687	3.918
6400	1.512944	12.415	12200	0.217647	3.882
6500	1.548294	12.268	12300	0.21664	3.882
6600	1.565965	12.195	12400	0.21664	3.882
6700	1.582629	12.158			
6800	1.587173	12.158			
6900	1.591213	12.158			
7000	1.593234	12.158			

7100	1.590207	12.122
7200	1.585153	12.122
7300	1.578086	12.122
7400	1.567482	12.122
7500	1.550314	12.122
7600	1.517991	12.122
7700	1.468501	12.122
7800	1.384674	12.122
7900	1.274585	12.122
8000	1.203383	12.122
8100	1.156423	12.122
8200	1.110973	12.122
8300	1.120564	12.122
8400	1.118543	12.158
8500	1.106429	12.122
8600	1.101375	12.122
8700	1.104409	12.122
8800	1.11047	12.122
8900	1.115013	12.122
9000	1.117537	11.169
9100	1.119557	9.851
9200	1.12006	8.569
9300	1.121074	7.214
9400	1.121577	5.933
9500	0.738291	5.127
9600	0.741324	5.054
9700	0.749398	5.054
9800	0.755969	5.017
9900	0.760512	5.017
10000	0.762022	5.017
10100	0.763539	5.017

### Experimental Results for Bending -Full Process

Time (ms)	Press. N/mm <sup>2</sup>	Displ. (mm)			
			5700	0.794848	27.869
0	0.530745	86.243	5800	0.798385	27.869
100	0.069685	86.279	5900	0.510543	28.235
200	0.069182	86.243	6000	0.268151	31.055
300	0.069182	86.243	6100	0.256533	33.911
400	0.069685	86.279	6200	0.264614	36.584
500	0.108572	86.243	6300	0.262594	39.478
600	0.242895	86.206	6400	0.261077	42.224
700	0.523671	86.023	6500	0.262594	44.971
800	0.928165	85.913	6600	0.26209	47.681
900	1.549804	85.4	6700	0.25956	50.61
1000	1.055422	83.716	6800	0.255016	53.32
1100	1.108449	82.544	6900	0.25401	56.104
1200	1.171068	81.299	7000	0.25401	58.85
1300	1.172074	80.017	7100	0.248453	61.56
1400	1.170557	78.735	7200	0.246432	64.343
1500	1.173591	77.49	7300	0.246432	67.2
1600	1.176115	76.062	7400	0.242392	69.946
1700	1.177631	74.817	7500	0.242392	72.766
1800	1.180155	73.499	7600	0.245426	75.476
1900	1.182175	72.18	7700	0.242895	78.296
2000	1.184195	70.898	7800	0.241889	81.079
2100	1.184699	69.58	7900	0.243909	83.862
2200	1.186215	68.262	8000	0.252493	86.646
2300	1.187732	66.98	8100	0.199472	87.305
2400	1.190256	65.625	8200	0.188868	87.305
2500	1.190759	64.307	8300	0.190378	87.341
2600	1.191773	62.988	8400	0.191392	87.341
2700	1.191773	61.67	8500	0.192398	87.305
2800	1.191773	60.352	8600	0.193412	87.305
2900	1.191773	59.07	8700	0.193915	87.341
3000	1.192276	57.788	8800	0.194418	87.341
3100	1.192779	56.506	8900	0.194922	87.341
3200	1.193793	55.188	9000	0.194922	87.341
3300	1.193793	53.87	9100	0.194922	87.341
3400	1.194296	52.551	9200	0.193915	87.341
3500	1.193793	51.233	9300	0.193412	87.341
3600	1.194296	49.915	9400	0.193412	87.341
3700	1.194296	48.56	9500	0.192908	87.341

3800	1.194799	47.241	9600	0.192908	87.341
3900	1.193793	45.923	9700	0.192908	87.341
4000	1.194799	44.641	9800	0.191895	87.341
4100	1.19682	43.359	9900	0.191392	87.341
4200	1.197826	42.041	10000	0.189875	87.341
4300	1.197826	40.759	10100	0.188868	87.341
4400	1.197323	39.478	10200	0.187855	87.341
4500	1.196316	38.123	10300	0.186338	87.341
4600	1.19682	36.768	10400	0.185331	87.378
4700	1.195813	35.449	10500	0.184318	87.378
4800	1.195813	34.167	10600	0.182808	87.378
4900	1.19682	32.849	10700	0.182808	87.378
5000	1.197323	31.567	10800	0.183311	87.378
5100	1.19884	30.249	10900	0.182808	87.378
5200	1.20086	28.967	11000	0.182808	87.378
5300	0.885749	27.905	11100	0.182297	87.378
5400	0.774654	27.832	11200	0.182297	87.378
5500	0.784244	27.869			
5600	0.790305	27.832			
11300	0.181794	87.378			
11400	0.181291	87.378			
11500	0.181794	87.378			
11600	0.181794	87.378			
11700	0.181794	87.378			
11800	0.181291	87.378			
11900	0.181291	87.378			
12000	0.182297	87.378			
12100	0.182297	87.378			
12200	0.183814	87.378			
12300	0.183814	87.378			
12400	0.184318	87.378			